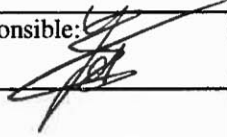


GEOLOGI FOR SAMFUNNET

GEOLOGY FOR SOCIETY



Report no.: 2014.041		ISSN 0800-3416	Grading: Open	
Title: Modelling water content and soil temperature in unsaturated urban deposits at Bryggen, Bergen				
Authors: Anna Seither		Client: Norges Forskningsråd, Riksantikvaren		
County: Hordaland		Commune: Bergen		
Map-sheet name (M=1:250.000) Bergen		Map-sheet no. and -name (M=1:50.000) Bergen, 1115 I		
Deposit name and grid-reference: Bryggen		Number of pages: 49	Price (NOK): 150,-	
Fieldwork carried out: -		Date of report: 04.12.2014	Project no.: 347500	Person responsible: 
Summary:				
<p>As a result of a lowered groundwater level and increased access of atmospheric oxygen, the organic archaeological deposits of Bryggen in Bergen, Norway, are in places strongly threatened to decompose. Besides degradation of the protected archaeological deposits, another negative outcome of this is that numerous of the wooden houses built on these cultural deposits settle at alarming rates. Major efforts were and are necessary to counteract this process and to save the World Heritage Site.</p> <p>As part of the <i>Cultural Heritage and Water Management in Urban Planning</i> (Urban WATCH) project, and with financial support of the Directorate for Cultural Heritage (Riksantikvaren) and the Research Council of Norway (Norges Forskningsråd), a soil-water storage model for a testpit at Nordre Bredsgården at Bryggen was constructed. A main objective was to investigate, to what extent existing data and measured time series can be used as model input to gain additional knowledge about relevant hydraulic processes at the site. A 3.5 m deep soil profile, parameterized with data from field and lab investigations, presented the core of the model. The water balance components of this profile were explored with the open source software CoupModel. Meteorological data from the station Bergen-Florida, and a time series of measured groundwater level in close proximity to the testpit, served as driving variables. Continuous measurements of soil temperature and water content in several depths were used for calibration.</p> <p>The model performed well in reproducing measured temperature series, but relatively weak in reproducing corresponding series of water content. The main reason for the latter is thought to be the heterogeneity of the urban site and the type of soil data available for parameterization. Future studies at similar sites are recommended to apply a sensor-pairing method for the determination of a soil water characteristic curve. Nevertheless, a few approximations could be made. According to storage simulations, the total water storage in the soil can vary more than 150 mm between summer and winter, corresponding to 150 L/m². The soil drains on average approximately 3 mm/day, but there are large differences between the summer and winter months. In order to protect the organic deposits from drying out during summer, the loss of water must be compensated. According to the conducted simulations, at least 0.08 L of water per hour and m² of soil must be injected to counterbalance the deficit.</p>				
Keywords: Groundwater		Cultural deposits		
Archaeology		CoupModel		
Unsaturated zone		Bryggen		

CONTENTS

1. INTRODUCTION.....	7
2. STUDY SITE	9
3. MATERIALS AND METHODS	10
3.1 Software.....	10
3.2 Soil data used for parameterization	10
3.2.1 Data from previous surveys.....	10
3.2.2 Grain size distribution	10
3.3 Driving variables	11
3.3.1 Meteorological data.....	11
3.3.2 Groundwater level	11
3.4 Validation data - monitored soil water content and soil temperature.....	12
3.5 CoupModel setup, parameterization and calibration.....	14
4. RESULTS AND DISCUSSION	18
4.1 Modelling performance	18
4.1.1 Soil temperature simulations.....	18
4.1.2 Water content simulations.....	21
4.2 Water balance	25
4.3 Evaluation of errors and model constraints	29
5. Recommendations	31
6. References	32
APPENDIX.....	34

FIGURES

Figure 1: Silhouette of Bryggen`s ancient timber houses. Photo: A. Seither.....	7
Figure 2: The harbor area of Bergen, Norway. The World Heritage Site Bryggen is located at the red marking. Photo extracted from www.norgebilder.no	9
Figure 3: Map of Bryggen, highlighting the sheet piling of the Royal Raddison SAS Blu hotel as well as the position of the testpit and the two closest observation wells, MB7 and MB21.....	9
Figure 4: Monthly normal values regarding precipitation and air temperature at the meteorological station Bergen-Florida (Station no.: 50540, Latitude 60.383, Longitude 5.3327, Elevation 12 m asl).....	11

Figure 5: Groundwater level in observation well MB21.....	12
Figure 6: Time series of the water content in six soil layers from January 2011 to December 2013 (Source: Nationalmuseet Denmark).....	12
Figure 7: Time series of measured soil temperature in different depths from January 2011 to December 2013 (Source: Nationalmuseet Denmark).	13
Figure 8: Model setup scheme of the mass balance. Crossed out components were not included.	15
Figure 9: Measured and modeled temperature at the soil surface (upper graph) and the top 10 cm of the soil profile.	19
Figure 10: Simulated snow depth and lower boundary of frost bodies.....	20
Figure 11: Number of days with soil temperatures below 0 °C.....	20
Figure 12: Comparison of soil surface temperature and air temperature. Except when snow covers the surface, air and soil surface temperature were set equal.	20
Figure 13: Mean values and extreme values for the warmest and coldest yearly soil temperatures in the soil profile (2007-2013).....	21
Figure 14: Measured and modeled water content in the top 10 cm of the soil profile for the years 2011 - 2013.	22
Figure 15: Measured and modeled water content in backfill material in a depth of about 40 cm in spring 2011.....	23
Figure 16: Measured and modeled water content in cultural deposits in a depth of about 1 m.....	24
Figure 17: Measured and modeled water content in the lime/sand layer in a depth of about 1.2 m.....	24
Figure 18: Validation of the modeled water content in the lower cultural deposits.	25
Figure 19: Simulated percentage of precipitation that evaporates, runs off, or infiltrates and drains in individual years from 2007 to 2013.....	26
Figure 20: Corrected precipitation, simulated infiltration and evaporation from April 2011 to December 2013.	26
Figure 21: The total difference in water storage (mm) in the soil profile from 2007 to 2013 (upper graph), with January 2007 being the reference point. The lower graph shows the changes in water storage (mm) together with the drainage flow rates (mm/day) for the last two years of the modeling period.	27
Figure 22: Monthly average values for evaporation (mm/day), drainage (mm/day) and the total difference in storage (mm) compared to January 2007. In order to visualize the effect of increased infiltration in the last 1.5 years on average values, two different periods are compared.	28

TABLES

Table 1: Performance indicators r^2 , mean error (ME) and Root Mean Square Error (RSME) for the comparison of simulated and measured soil temperature in different depths.	18
Table 2: Performance indicators r^2 , mean error (ME) and Root Mean Square Error (RSME) for the comparison of simulated and measured soil water content in different depths.	22
Table 3: The averaged changes in water storage in the soil (mm) in 2007-2013. Negative values indicate overall loss of water from the soil during that period, while positive values indicate replenishment.	28

APPENDIX

Tables

Table A 1: Soil samples collected 3.4.2013 in between the testpit US1 and the observation well MB21.	34
Table A 2: Sample weights and soil water content	35
Table A 3: Cumulative grain size distribution and coefficients of uniformity for the < 2 mm fraction	35
Table A 4: Clay (< 2 μm) , silt (2-60 μm) , sand (0.06-2 mm), and gravel fractions (> 2 mm) of the soil samples	36
Table A 5: General information, model structure, technical and numerical settings.....	36
Table A 6:Parameter values at investigated horizons used for retention and conductivity calculations.....	36
Table A 7: Switches and parameter settings with respect to meteorological data, radiation properties and soil evaporation.	37
Table A 8: Switches and parameter settings with respect to soil and surface water.....	38
Table A 9: Snow and frost settings and parameters.	39
Table A 10: Soil thermal and heat flow settings and parameters.	40
Table A 11: Linear regression values (r^2 , intercept and slope), Mean Error values (ME), and Root Mean Error Values (RMSE) for the comparison of simulated and measured soil temperatures and water contents.	40
Table A 12: Soil cover dynamics	41
Table A 13: Hysteresis effects in different depths	41

Figures

Figure A 1: Overview about the grain size distributions of the fine soil fractions	42
Figure A 2: Grain size distribution curve of soil sample 1. Texture class Sandy loam.	43
Figure A 3: Grain size distribution curve of soil sample 2. Texture class Loamy sand	43
Figure A 4: Grain size distribution curve of soil sample 3. Texture class: Loamy sand.	43
Figure A 5: Grain size distribution curve of soil sample 4. Texture class: Sandy loam.	44
Figure A 6: Grain size distribution curve of soil sample 5. Texture class: Loam.....	44
Figure A 7: Grain size distribution curve of soil sample 6. Textural class: Loamy sand	44
Figure A 8: Grain size distribution curve of soil sample 7. Textural class: Loamy sand	45
Figure A 9: Grain size distribution curve of soil sample 8. Textural class: Sandy loam.....	45
Figure A 10: Grain size distribution curve of soil sample 9. Textural class: Loamy sand	45
Figure A 11: Grain size distribution curve of soil sample 10. Textural class: Sandy loam.....	46
Figure A 12: Measured and modeled soil temperature at a depth of 0.3 - 0.4 m.....	46
Figure A 13: Measured and modeled soil temperature at a depth of 0.5 - 0.6 m.....	47
Figure A 14: Measured and modeled soil temperature at a depth of 0.7 - 0.8 m.....	47
Figure A 15: Measured and modeled soil temperature at a depth of 0.9 - 1.0 m.....	48
Figure A 16: Measured and modeled soil temperature at a depth of 1.2 - 1.3 m.....	48
Figure A 17: Measured and modeled soil temperature at a depth of 1.4 - 1.5 m.....	49
Figure A 18: Measured and modeled soil temperature at a depth of 1.6 - 1.7 m.....	49

1. INTRODUCTION

Among tourists, the city of Bergen in Norway (60.4°N, 5.3°E) is best known for its historic timber buildings at the World Heritage Site Bryggen. For most visitors however, it goes unnoticed, that the buildings rest on up to 10 m of thick, organic rich, cultural deposits. A part of the area was excavated in the 50s and 60s. It revealed outstanding archaeological artefacts out of wood, leather, bone and plant material. These deposits are a non-renewable, archaeological resource, and are as such, protected.

However, recent years have shown that preservation conditions have deteriorated considerably in parts of the area. The organic materials in the cultural layers started to decay, which in turn led to settling of the protected buildings above. According to Jensen (2007), buildings at



Figure 1: Silhouette of Bryggen's ancient timber houses. Photo: A. Seither

the Bredsgården and Bugården settle at an alarming rate of up to 6-8 mm/year. The ongoing decomposition and subsequent settling appears to be caused by a lowered and highly variable groundwater table in the area (De Beer, 2008; De Beer & Matthiesen, 2008). With a long-term average of 2250 mm precipitation per year, there is no shortage of water in Bergen. However, sealed soil surfaces, collection of runoff in storm sewer systems, artificial drainage, and local pumping activities, led to critically low groundwater levels in several vulnerable areas. A low groundwater table facilitates the access of atmospheric oxygen into the soil and leads to increased decay of the organic materials.

Cultural heritage protection is an integral part of Norway's *Directorate for Cultural Heritage (Riksantikvaren)*. In order to counteract the loss of archaeological valuable materials and the destructive effects of settling, Riksantikvaren started off with the preservation programme "Prosjekt Bryggen" (Project Bryggen). Since 2001, when the project began, the funding for research and site remediation has gradually increased.

In 2012, the *Cultural Heritage and Water Management in Urban Planning (Urban WATCH)* project was initiated. It is a collaborative project between NGU, NIVA, NIKU, NIBR, the National Museum of Denmark and the TU Delft and MVH Consult in the Netherlands. The project is partly financed by the *Research Council of Norway (Norges Forskningsråd)*, as part of the programme "Miljø2015" (Environment 2015).

Over recent years, vast amounts of data were collected at Bryggen and various measures to raise the groundwater level have been conducted. Anchor holes at the sheet piling of the hotel were sealed, compact cobblestone pavements were exchanged with gravel, roof water was infiltrated into the ground and swales were constructed. Collected data include archaeological descriptions, time series of the piezometric head in about 40 observation wells, as well as

chemical analyses and settling rates of the terrain and buildings. To better understand the preservation conditions in these complex surroundings, many of these data were applied in a 3D subsurface model and a groundwater flow model of the area (de Beer et al., 2012).

The installation of a testpit with monitoring equipment, that registers soil water content and temperature in different depths of the unsaturated zone, enabled the construction of another kind of model - a soil-water storage model with the open source software CoupModel. The modelling was performed as part of the Urban WATCH project and with funding of both the Riksantikvaren and the Forskningsrådet.

To the best of our knowledge, it has not been attempted to build such a model for an urban, archaeological soil before. Hence, one of the main objectives was to investigate, to what extent the collected data can be used as model input to gain additional knowledge about hydraulic processes at the site.

2. STUDY SITE

The study site is located in the historical harbour area Bryggen in Bergen (60.4°N, 5.3°E), Norway. The aerial photo in Figure 2 gives an overview of the area and highlights the location of Bryggen. In 2006, monitoring equipment was installed in the unsaturated zone of the soil at Bredsgården (see Figure 3).

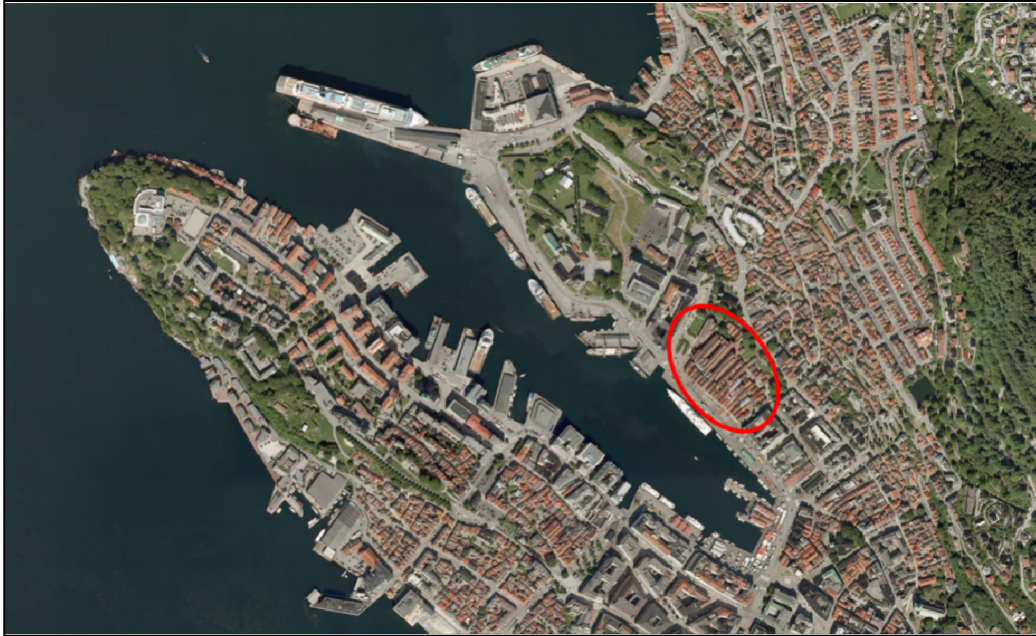


Figure 2: The harbor area of Bergen, Norway. The World Heritage Site Bryggen is located at the red marking. Photo extracted from www.norgebilder.no.

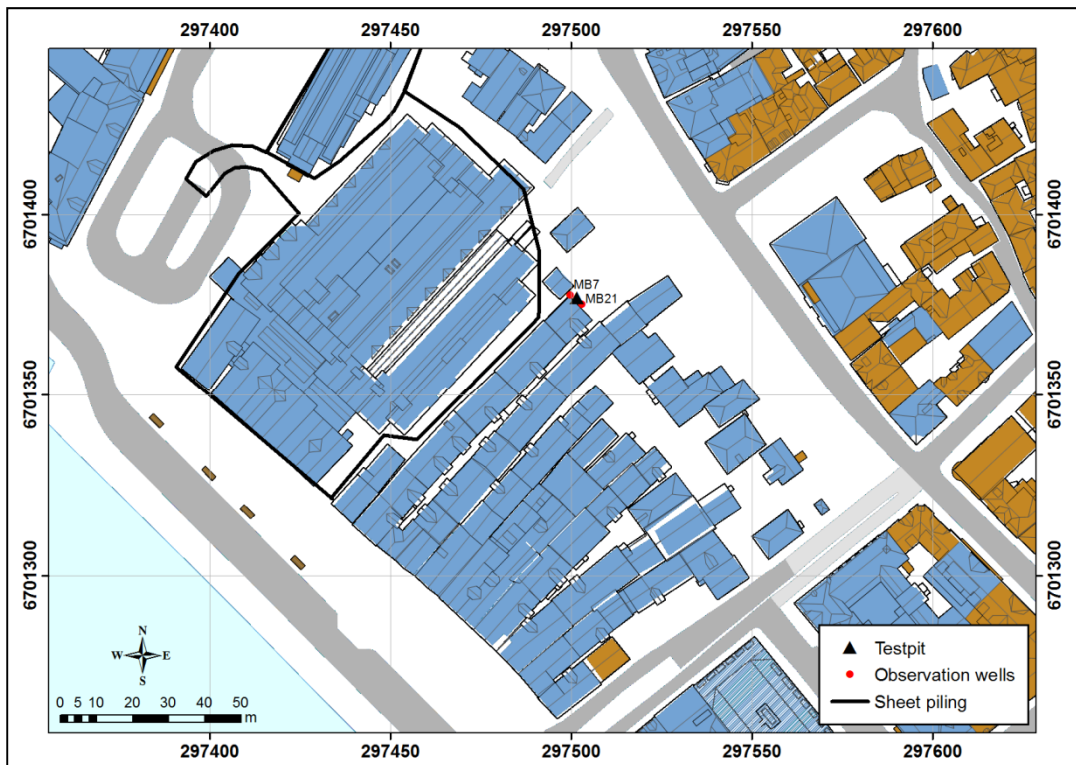


Figure 3: Map of Bryggen, highlighting the sheet piling of the Royal Raddison SAS Blu hotel as well as the position of the testpit and the two closest observation wells, MB7 and MB21.

3. MATERIALS AND METHODS

3.1 Software

The water balance components of the soil profile at the testpit (Figure 3) were explored with the open source software CoupModel. It is a physically based model that simulates water and heat flux through a one-dimensional soil profile using a combination of the Richards and Fourier equation (Jansson 2012). The equations are solved with an explicit numerical method. CoupModel comprises a substantial range of sub-modules, such as infiltration, evapotranspiration, heat storage, soil frost, crop growth, and C/N cycle. Depending on the study objectives and the available data, suitable modules can be combined.

3.2 Soil data used for parameterization

3.2.1 Data from previous surveys

In 2006, a 2.5 deep testpit was opened at the northern end of Bredsgården. The state of preservation of the cultural deposits was assessed (Dunlop 2008), water content sensors and modern wood samples were installed before refilling the testpit. Observations and results are discussed in Matthiesen (2007, 2010) and Matthiesen et al. (2008). The testpit was re-opened in 2010, in order to retrieve soil samples and the introduced wood samples, and to install further monitoring equipment. The report of Matthiesen and Hollesen (2011) describes the results of the field measurements and laboratory analyses, such as loss on ignition and porosity. These values, as well as the descriptions given in Dunlop (2008) were the basis for the parameterization of the soil profile.

3.2.2 Grain size distribution

Additional soil sampling was necessary to supplement existing data of soil layers in the testpit US1 located in Nordre Bredsgården, Bergen. However, re-opening the monitored testpit would lead to major disturbances of logger data. Accordingly, the drill core was taken in between site US1 and MB21 instead. Due to disturbances, the upper 60 cm could not be sampled. Total drilling depth was approximately 3 m.

The ten samples are considered to be representative for the local subsurface. It was attempted to relate them to previous samples from the nearby testpit. However, the identified sequences were not identical and the degree of discrepancy is unclear. Detailed information about sampling depths and layer affiliation is given in the Appendix (Table A 1).

After a visual inspection, soil samples were frozen and dried by sublimation using a freeze drier. Gravimetric soil moisture content was determined by weighing the samples before and after drying. The samples were kept at room temperature and stored in plastic bags.

All ten soil samples were subject to a textural analysis at the NGU laboratory. After homogenization, a proportion of the samples was taken into beakers, suspended in tap water, and oxidized using 30% H₂O₂. Excess solution was evaporated, followed by freezing and dry-freezing of the samples. The grain size distribution above 2 mm was determined manually by sieving and weighing. The proportion below 2 mm was investigated using a Beckman Coulter counter LS 200. Assuming spherical particles, the method provides data with an uncertainty of ± 10 wt% (cumulative). Graphs and tables presenting the results of the grain size distribution analyses are given in Figure A 1 - Figure A 11, Table A 3 and Table A 4 in the appendix.

3.3 Driving variables

3.3.1 Meteorological data

Meteorological data from the station Bergen-Florida in the city centre served as driving variables for the model. Long-term observations (1961-1990) show an annual average temperature of 7.6 °C and a precipitation of 2250 mm per year. Measurement data of precipitation, air temperature, vapour pressure, and cloud cover were obtained at a height of 2 m from the weather station. Figure 4 shows climate normals for Bergen.

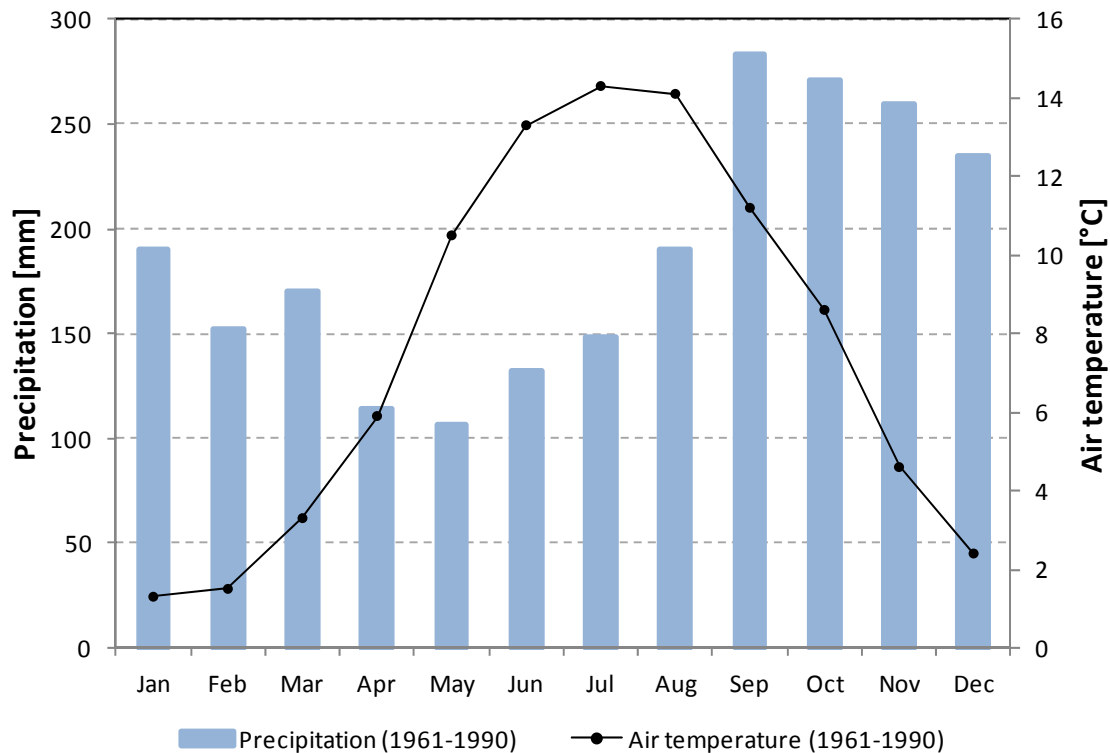


Figure 4: Monthly normal values regarding precipitation and air temperature at the meteorological station Bergen-Florida (Station no.: 50540, Latitude 60.383, Longitude 5.3327, Elevation 12 m asl).

Wind speed and snow depth data were available as well, but since the testpit is located in about 2 km distance from the station and shielded by several buildings, measurements were considered to be not representative for the site.

3.3.2 Groundwater level

The time series of groundwater level in the nearby observation well MB21 (Figure 5) could either be used for validation purposes or as lower boundary condition of the soil profile. Due to the large variations and sudden changes in saturation depth, it was decided to use the groundwater level data as a driving variable.

As seen in (Figure 5), “cut-off” values occur at a depth of approximately 2.9 m during the first two years. The sensor had not been installed deep enough in the well and fell dry during drier periods. The position of the sensor was adjusted as soon as the problem was noticed.

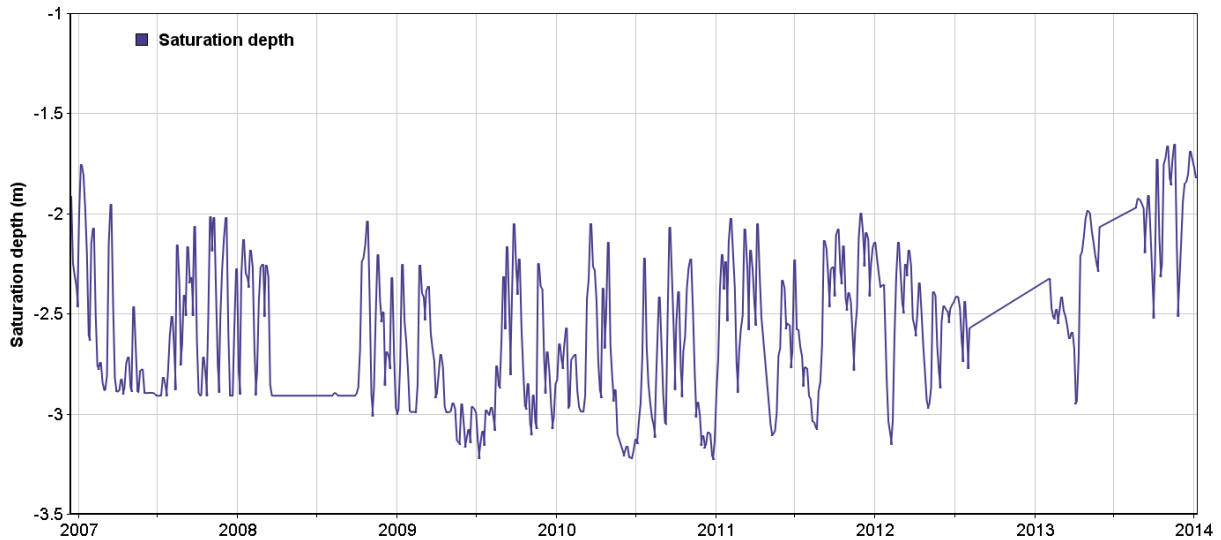


Figure 5: Groundwater level in observation well MB21

3.4 Validation data - monitored soil water content and soil temperature

In 2010, sensors for water content and soil temperature were installed in different soil layers and connected to a data logger, which reports measured data every 30 min. For more information about equipment and measurements, see Matthiesen & Hollesen (2011). The graph in Figure 6 shows the registered time series for water content from October 2010 to December 2013. Generally spoken, the water content increases and its variation smoothens with depth. The only exception is the gravely layer at a depth of about 2.3 m asl (grey curve). It lies between two layers with entirely different hydraulic properties.

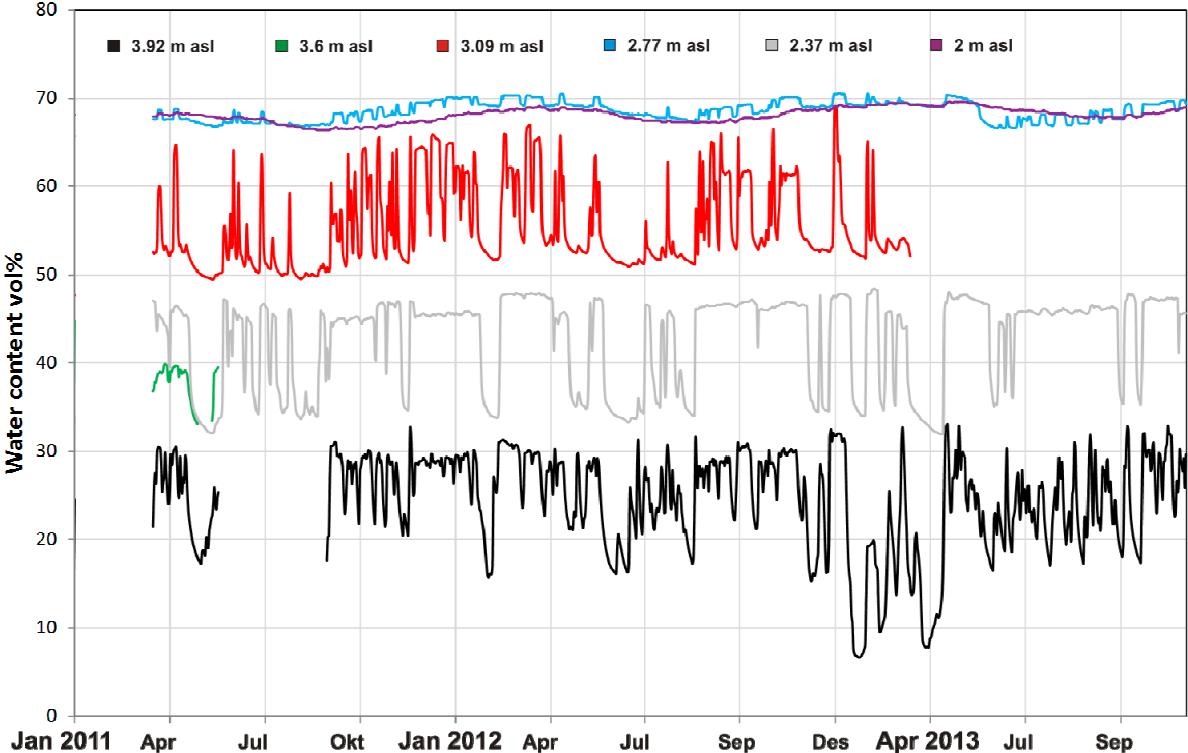


Figure 6: Time series of the water content in six soil layers from January 2011 to December 2013 (Source: Nationalmuseet Denmark).

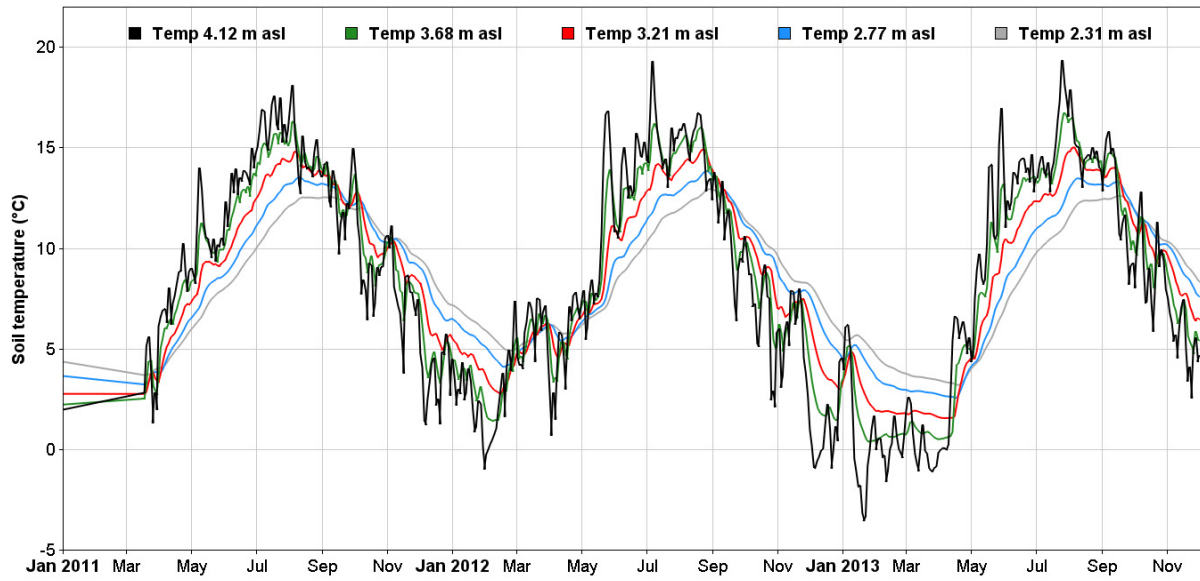


Figure 7: Time series of measured soil temperature in different depths from January 2011 to December 2013 (Source: Nationalmuseet Denmark).

3.5 CoupModel setup, parameterization and calibration

The CoupModel comes with a variety of additional submodels to describe particular processes in the soil profile and a very long list of input parameters. These submodels were tested for their suitability and the general impact of individual parameters was investigated thoroughly. The sensitivity analysis identified influential settings and parameters. In order to keep the model as simple as possible, functions that added model complexity without influencing model performance were left out.

The core of the model is a 3.5 m deep soil profile that was parameterized according to field and lab investigations. Figure 8 provides an overview over the model setup. It visualizes not only the mass balance components that were included into the model, but also those that were not incorporated. The soil surface presents the upper boundary of the model, where water enters and leaves the soil profile by precipitation and evaporation. CoupModel is regularly used to simulate soil-water-plant dynamics. But since the profile is located in an urban setting, in-between houses and underneath cobblestone, vegetation is entirely left out of the model. It was assumed, that the transport of mass and energy is mainly vertical, with drainage being the only exception. There is no lateral input of soil water into the profile.

Drainage in the model followed the physical drainage equation after Hooghoudt (1940). The lower boundary, the bottom of the profile was considered to be entirely “waterproof” and any drainage occurred horizontally to drainage pipes only. The drainage level was forced to follow the daily mean variations of the groundwater level in observation well MB21. Return flow was included in order to improve the fitting.

Meteorological data from the station Bergen-Florida in the city centre served as driving variables for the model. The data were loaded with a resolution of daily mean values and the model was run with 96 iterations per day. The rate and quantity of **soil evaporation** is a complex process that is affected by many interacting factors such as solar radiation, air temperature, air humidity, wind speed, and soil characteristics. The CoupModel user may choose between an explicit energy balance approach (EBAL), and an implicit approach using the Penman-Monteith equation (PM). According to Jansson (2012), EBAL generally shows better results regarding soil temperature dynamics, whereas PM often gives a better description of soil moisture dynamics. As the focus of the whole project lies on water, the empirical PM approach, combined with a simple function for the surface resistance of the soil, was chosen to calculate soil evaporation. This approach determines evaporation using the energy that is available at the soil surface and the aerodynamic and surface resistances. Because the meteorological station Bergen-Florida does not measure **net radiation**, a time series was estimated by the equation after Konzelmann et al (1994), using two separate formulas for incoming and out-going long-wave radiation. The parameters **air temperature** and **vapour pressure** were supplied as time series. The relative **duration of sunshine** was deducted from the cloud cover, **surface temperature** of the soil was defined to equal air temperature, and global short-wave radiation was estimated with default settings. Due to the lack of representative **wind speed** data, a time series with a constant wind speed of 2 m/s was generated.

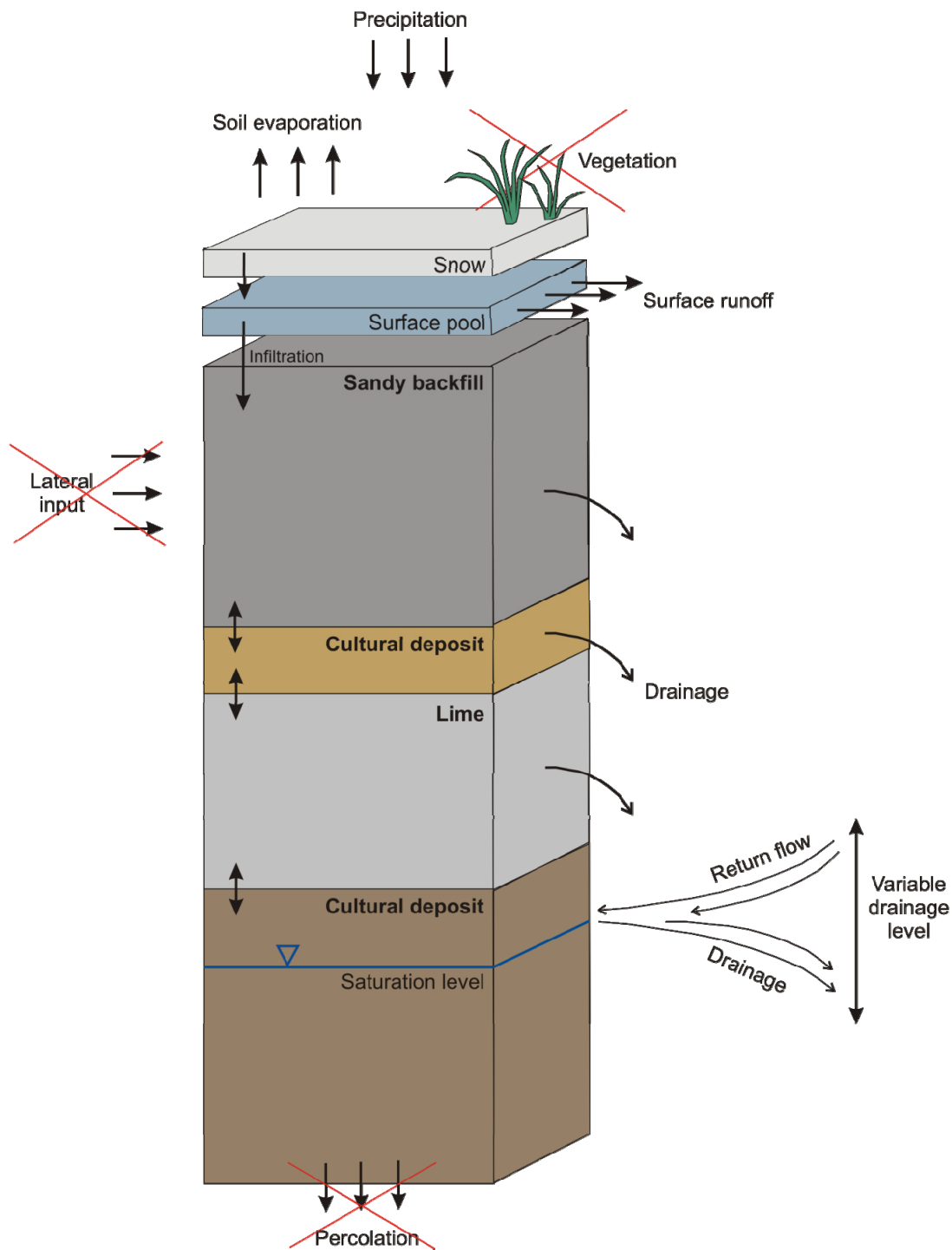


Figure 8: Model setup scheme of the mass balance. Crossed out components were not included.

When simulating soil water- and heat-processes for Norwegian sites, **snow and frost dynamics** should be included in the model. Snow stores water above ground and leads to delayed infiltration. Soil frost on the other hand reduces the liquid water content of a soil layer and influences the percolation of water through the profile. Snow fall was generated in dependence of the air temperature at which the precipitation occurred. Above 2°C, precipitation was considered to consist of rain only. Precipitation occurring between 0°C and 2°C came down as sleet. Any precipitation at air temperatures below 0°C was modeled to be pure snow. All options regarding the density of newly fallen snow, subsequent densification, snow melt and all respective parameters were kept to the default settings. Soil frost was allowed to influence water.

The inclusion of vapour flow in the soil did not change the performance very much (relevant at the third/fourth digit after the comma of r^2 values), so the simulations were conducted without it. The simulation of a soil-water barrier, as well as the simulation of convective gas flow, deteriorated model performance for all soil horizons, so these switches were turned off, too. However, the consideration of both hysteresis (values listed in Table A 13) and preferential flow paths led to a better fit of modeled and measured soil water content.

All model parameters except for soil cover were kept constant during the simulations. In order to account for gradually improved infiltration over the simulation period, the initial value of 60% soil coverage was successively reduced to 0% (details in Table A 12).

The **soil array** was defined as a vertical array of 35 layers, each with a thickness of 0.1 m and distinct hydraulic properties. Within the compartments, all properties as well as subsequent modelling results are considered to be constant. Initially, the properties of seven soil layers with a combined depth of 2.2 m were used to estimate values for the soil array. The model then used the input values to interpolate parameter values for each model slice. However, using seven layers proved to be too detailed.

Figure 6 in chapter 3.4 shows a general increase of the water content as well as a gradual smoothing of the curves with depth. Only the gravel layer in about 1.5 m depth does not fit into that observation. Its grain size distribution differs considerably from the ones of its neighbouring layers. It has a lower porosity, a high portion of macropores and hardly any organic materials. Accordingly, small water content changes in the surrounding layers have a big impact on the gravel layer. Its water content changes dramatically over time. Considering that the two neighbouring layers are relatively similar to each other, the gravel layer only complicated the modelling process, without increasing the informative value of the model itself. Therefore, the gravel layer was removed from the model and not considered at all. Altogether, five layers with distinct properties (appendix, Table A 6) were defined.

The grain size distribution and porosity of the soil served as basis to estimate hydraulic properties such as air-entry and residual water using the Brooks & Corey (1964) as well as the Mualem equations (Mualem, 1976). However, since these equations do neither account for the effect of organic materials nor for that of stones, very decisive characteristics of soils at Bryggen are not accounted for. Soils underneath Bryggen are not only highly organic, but the organic materials themselves are of varying origin and possess a varying degree of degradation. These inhomogeneities and uncertainties challenged the estimation of soil hydraulic properties considerably. The layers were initially parameterized with estimated hydraulic properties derived from the grain size distribution, but modelling with these values gave poor results.

Due to the complexity and heterogeneity of the soil, appropriate literature values could not be found either. However, even though it was not possible to apply specific values that are given in other studies, their general conclusions about how organics and stones influence the hydraulic properties of a soil were used to modify the calculated properties into the right direction. Melling et al. (2007) showed for example, that water retention curves of peat can be shaped similar to those of clay loam, but with a higher volumetric water content under high matric suction. Another study (Rawls et al., 2003) demonstrated that the volume of soil organic matter has a larger effect on water retention at the water content close to field capacity than water retention close to the wilting point.

After sensitivity analysis, a **multirun calibration** with the Generalized Likelihood Uncertainty Estimation (GLUE) approach of Beven and Binley (1992) was conducted. The basic idea behind GLUE is that there is no unique optimum parameter set within a certain model structure. Instead, different parameter sets may produce similarly good fits. GLUE is

typically applied to non-linear systems, for which a unique calibration is not apparent. GLUE does not implement a statistically consistent error model, it requires subjective decisions on the likelihood function as well as on the cut-off threshold. Hence, uncertainty becomes a matter of subjective interpretation. The approach is therefore strongly criticized by Stedinger et al. (2008), but for the study on hand there were no suitable alternatives.

Theoretically, one large multirun with several ten thousand runs that considers numerous parameters with a reasonable parameter range could be conducted. However, multiruns with more than 500 runs frequently crashed and could not be completed. Accordingly, the calibration was done sequentially instead: A sequence of simulations was run with a plausible range of parameter sets for parameters such as pore distribution index, air entry tension, minimum conductivity value, and drain spacing - producing multiple sets of model output. The simulation errors were summarized with performance indicators, the simulations were compared and screened for acceptable solutions. The correlation of parameters was investigated and a new multirun, with adapted parameter ranges and new, additional parameters was conducted. It must be emphasized, that there was no individual run that gave the best performance for all validation series, but many parameter combinations that gave very similar results. The parameter values listed in Table A 6 – A 10, as well as the results presented in the next chapter, were extracted from one of the accepted simulations.

4. RESULTS AND DISCUSSION

4.1 Modelling performance

Model performance was evaluated by a variety of indicators, including the Pearson's coefficient of correlation r^2 . R^2 is a widely applied performance indicator, that describes how much of the observed variance between measured and modeled values can be described by the linear fit. However, the given simulation is highly non-linear and hence, a major requirement for a meaningful application of r^2 is not met and other performance indicators, such as the mean error ME, as well as the root mean square error (RMSE) were applied additionally. But also these indicators have their restrictions, so a subjective evaluation of the goodness of fit by visually comparing simulated and measured time series played a very important role as well.

4.1.1 Soil temperature simulations

The model performed well in reproducing the measured soil temperatures (Table 1). The coefficient of determination for the linear regression varies between 0.89 and 0.98. Slightly positive values for the mean error show that the soil temperature of the uppermost 40 cm was systematically overestimated, while the opposite was true for the remaining 3.10 m of the modeled soil profile. According to the Root Mean Square Errors (RMSE), the overestimation at the surface can be up to 1.9 °C. In intermediate depths of around 1 m, soil temperature may be underestimated by around 0.7 °C. Below depths of 1.70 m, the systematic underestimation of soil temperature increases to about 0.9 °C.

Table 1: Performance indicators r^2 , mean error (ME) and Root Mean Square Error (RMSE) for the comparison of simulated and measured soil temperature in different depths.

Height of sensor (m asl)	r^2	ME	RMSE
4.12	0.89	0.23	1.87
3.92	0.90	0.56	1.79
3.68	0.97	0.04	0.81
3.46	0.98	-0.04	0.68
3.21	0.98	-0.17	0.61
3.06	0.98	-0.22	0.71
2.77	0.97	-0.47	0.84
2.5	0.95	-0.49	0.86
2.31	0.92	-0.54	1.03

Figure 9 shows the comparison of measured and simulated temperature values at the soil surface and in the uppermost soil layer. The respective graphs of the remaining temperature sensors can be found in the appendix (Figure A 12 - Figure A 18). Temperatures below 0 °C were simulated to change the energy storage in the soil such that soil water is able to freeze in the model. According to these simulations, soil frost reaches depths of up to 54 cm (Figure 10). The number of days with soil temperatures below 0 °C varies strongly from winter to winter (Figure 11). A snow layer insulates covered soil from minus temperatures in the surrounding air. In order to account for this effect, the temperature of the soil surface was set equal to the air temperature except when an insulating layer of snow covered the surface (see Figure 12). Nevertheless, soil temperature during winter is partly underestimated, leading to more days of frost than registered and a presumably larger frost depth than in reality. This

might be due to the use of daily mean air temperature values, which could have changed the proportion of precipitation that was modeled to be rain, sleet or snow. The soil temperature deviations in winter (Figure 9) indicate that more precipitation came down as snow. Alternatively, the site may occasionally have an extra thick snow cover due to snow clearance on the nearby footpath.

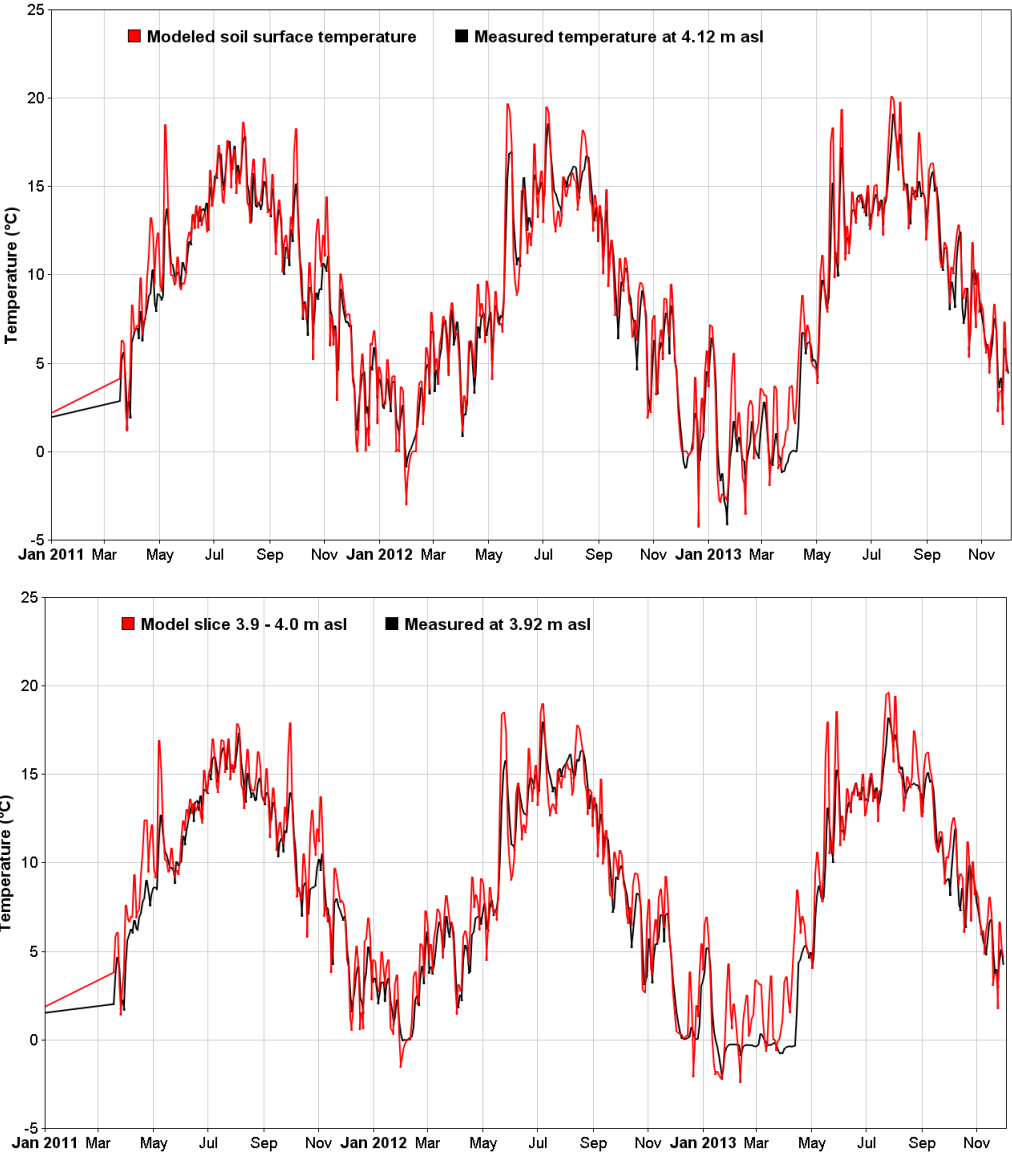


Figure 9: Measured and modeled temperature at the soil surface (upper graph) and the top 10 cm of the soil profile.

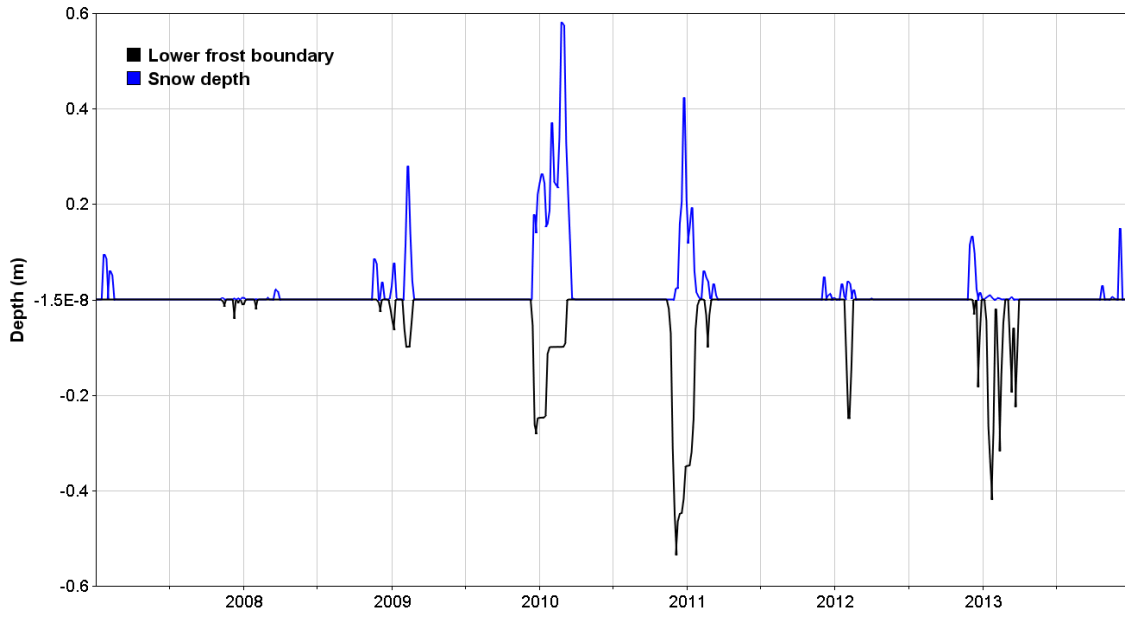


Figure 10: Simulated snow depth and lower boundary of frost bodies.

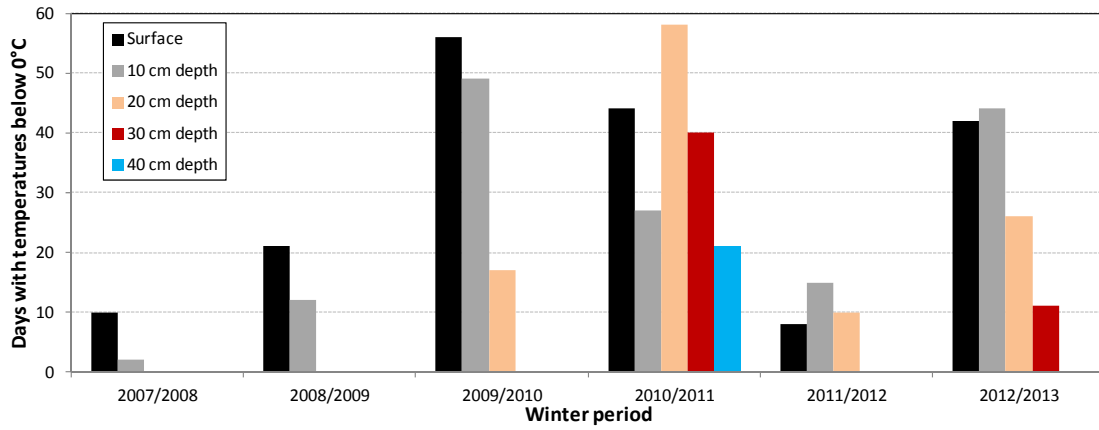


Figure 11: Number of days with soil temperatures below 0 °C.

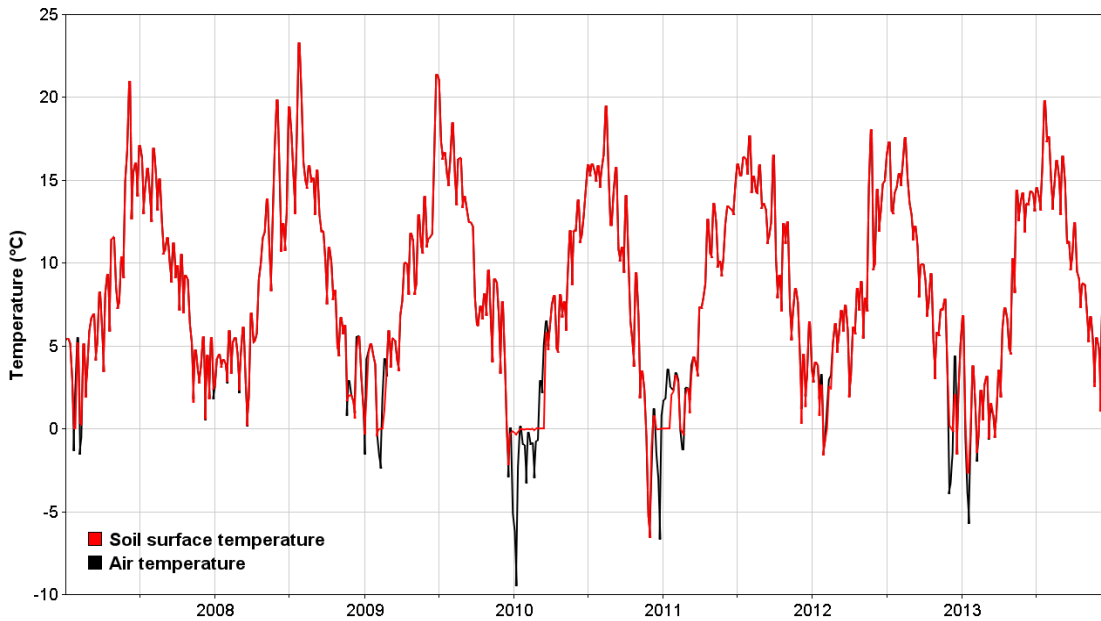


Figure 12: Comparison of soil surface temperature and air temperature. Except when snow covers the surface, air and soil surface temperature were set equal.

Figure 13 shows mean and extreme values for the warmest and coldest yearly soil temperatures in the whole soil profile. Based on the analysis above, the coldest values in the top soil were most likely overestimated. The mean values however, are thought to give a realistic picture of the soil temperature.

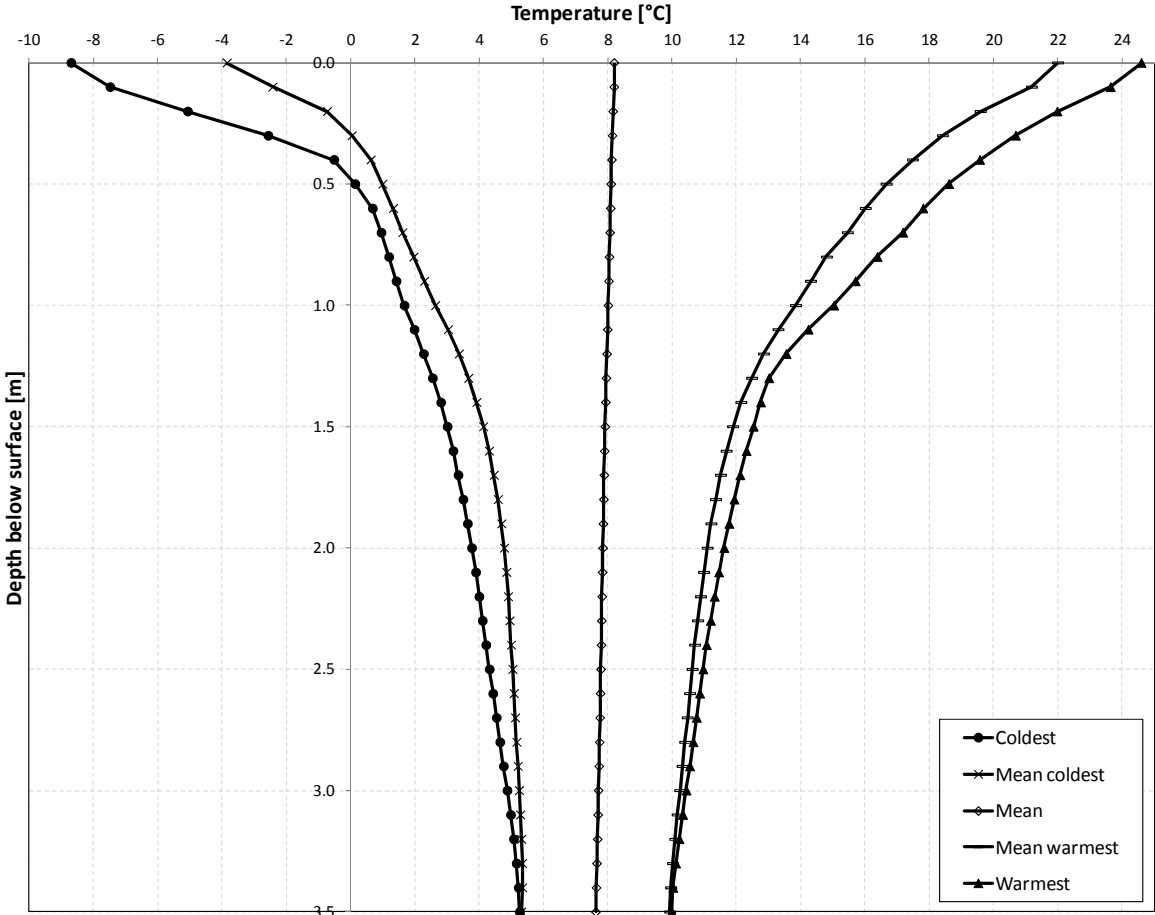


Figure 13: Mean values and extreme values for the warmest and coldest yearly soil temperatures in the soil profile (2007-2013)

4.1.2 Water content simulations

Overall, water content simulations reproduced measured time series rather weakly. The main reason for this is thought to be, that the kind of soil data used for the derivation of hydraulic properties are not suitable for simulation purposes of urban sites. In addition, the uncertainties arising from this issue are too large to undertake a fully satisfying calibration for the model. It is necessary to keep in mind, that not all horizons are equally important. First of all it was crucial to identify suitable settings for the upper and lower boundary of the soil profile. Accordingly, the volume of water that infiltrates during a given precipitation event should be as close to the actual infiltration as possible. Similarly, drainage from the unsaturated zone to the groundwater table had to be sized realistically. In between these boundaries, it is the water dynamics of the organic, cultural layers that are of interest. Surrounding layers of different composition are important for the description of the overall water balance of the profile, but individual deviations from measured values are considered to be of minor relevance.

Table 2: Performance indicators r^2 , mean error (ME) and Root Mean Square Error (RSME) for the comparison of simulated and measured soil water content in different depths.

Height of sensor (m asl)	r^2	ME	RMSE
3.92	0.49	0.78	5.11
3.6	0.05	-10.61	10.97
3.09	0.27	-1.62	4.57
2.77	0.36	-4.19	4.84
2	0.14	0.95	1.25

Figure 14 shows the comparison of measured and modeled water content values in the top 10 cm of the soil profile. The goodness of fit varies strongly over the monitored period. This is due to a combined effect of the parameters that were chosen for the upper part of the soil profile, and by physical changes at the surface over time. In 2012, the infiltrability of the pavement was improved, and it is difficult to assess, to which degree these activities might have physically altered the topsoil and hence modified its hydraulic properties. The improved infiltration was modeled by gradually removing a physical barrier covering the testpit. Soil properties however were kept constant.

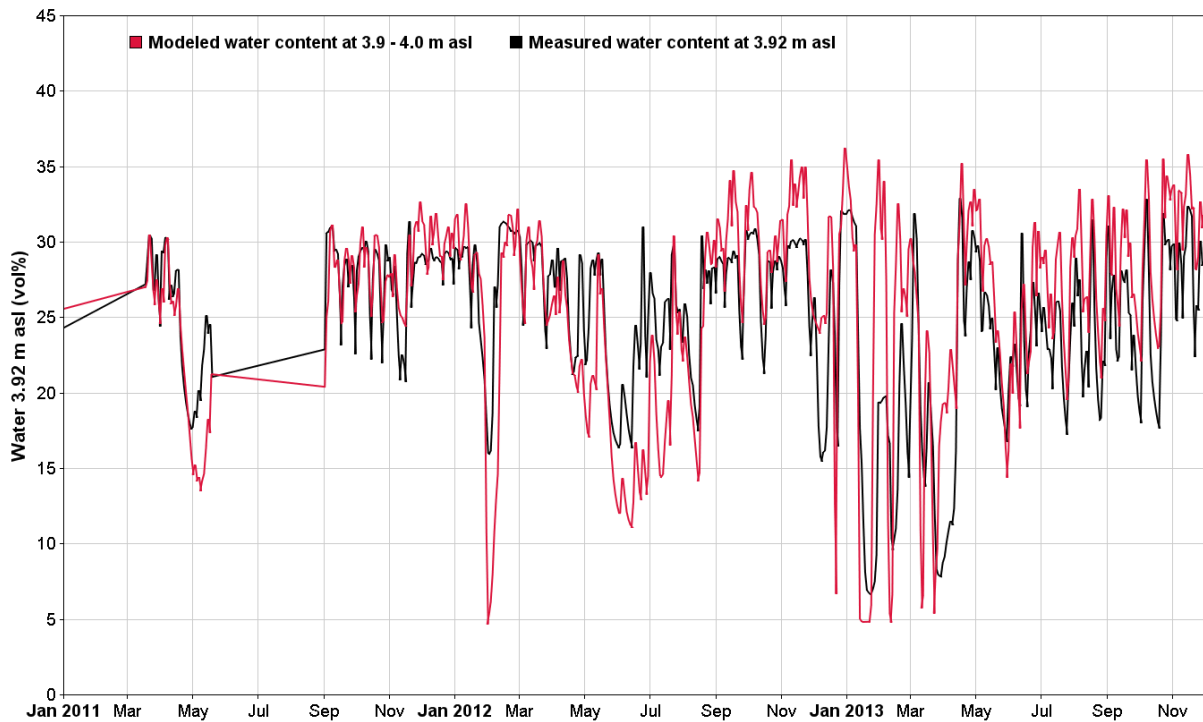


Figure 14: Measured and modeled water content in the top 10 cm of the soil profile for the years 2011 - 2013.

The steep drops in simulated as well as measured water content in both winter periods were caused by the presence of soil frost (see Figure 10), which temporarily removed soil water from the system. The large deviation in February 2012 was due to an erroneous estimation of the number of days with soil frost. Similarly, water content deviations the winter period 2012/2013 reflect uncertainties about the several frost periods. Following this observation, it could be suspected, that soil frost may not influence water flow at Bryggen after all. However, ignoring soil frost led to the other extreme. Sudden drops of the observed soil water content during winter could not be simulated without the consideration of soil frost and the overall performance for the upper 10 cm was instantly reduced from an r^2 of 0.49 to 0.3.

The time series of water content in backfill materials underneath the top layer was not used for calibration purposes. The respective model slices in the soil profile were not

parameterized with the aim to reproduce the water content values of these two months, but with the aim to improve the respective fitting of the layer above and the cultural deposits below. For the sake of completeness, the comparison between modeled and measured values of this horizon is shown in Figure 15. In the available time period, the soil water content is systematically underestimated by about 10 vol%.

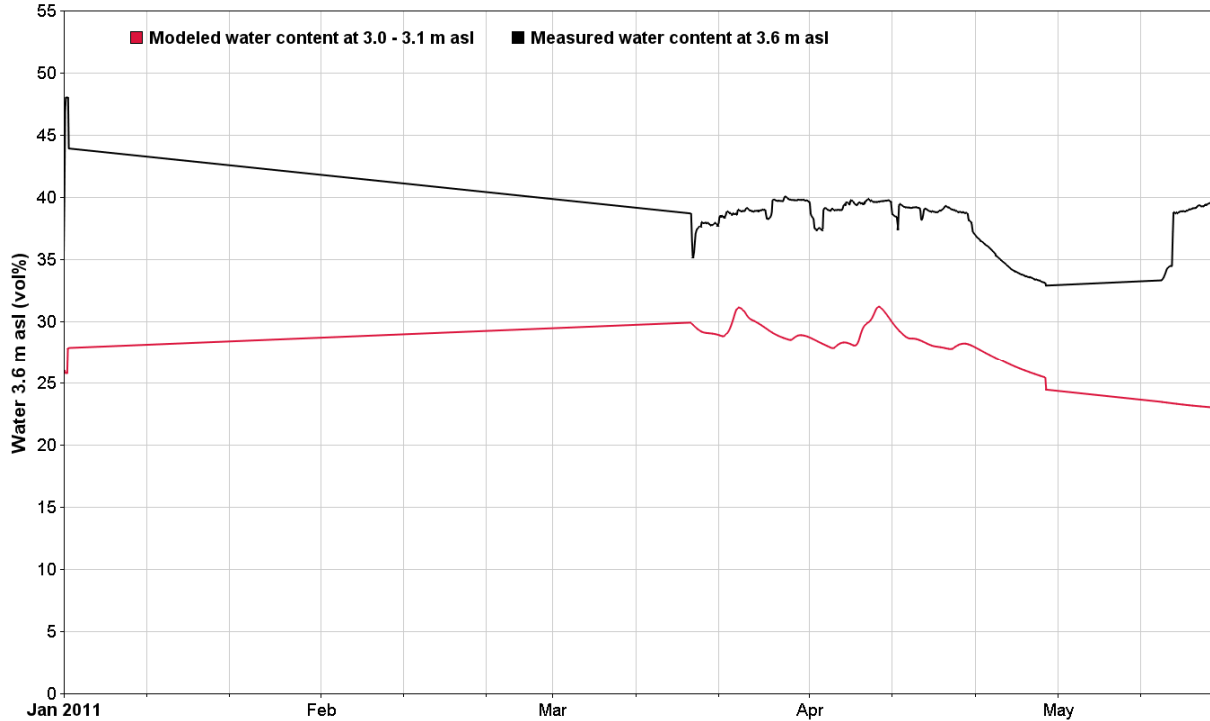


Figure 15: Measured and modeled water content in backfill material in a depth of about 40 cm in spring 2011.

The upper cultural layer shows a very distinct drying and wetting behaviour. According to measurements, it has a total porosity of 62 vol%. However, according to monitoring data of the water content, the horizon reaches water contents of about 70 vol% (see Figure 16). This may partly be caused by major inhomogeneities of the soil and different types (sedimentary, fibrous, woody etc) of organic materials. However, it may also indicate swelling, which is a common trait of organic soils. If the porosity measurements are correct, the soil is regularly oversaturated. Water content near saturation changes quickly with changes in pressure, but there seems to be a lower baseline slightly above 50 vol%, where the water content stabilizes. The r^2 of the linear fit was 0.27, and the combined interpretation of the mean error and the RMSE indicates a systematic underestimation of about 5 vol%. The model does not account for the high and steep peaks in water content, but it follows the same base line and reflects thereby the general trend of the dynamics.

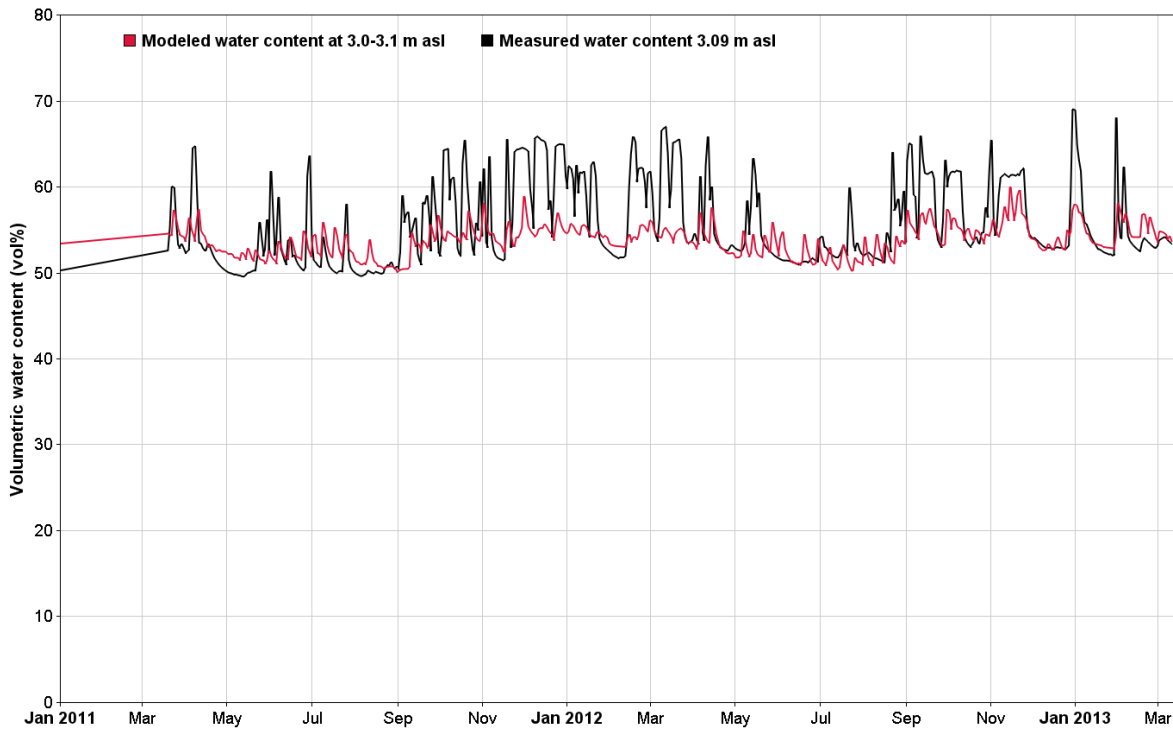


Figure 16: Measured and modeled water content in cultural deposits in a depth of about 1 m.

The sandy lime layer in a depth of about 1.2 m has a constantly high water content near 70 vol%. The r^2 of 0.36 indicates a weak, linear fit. Both a visual interpretation and a mean error of -4.2 show, that the water content is generally underestimated.

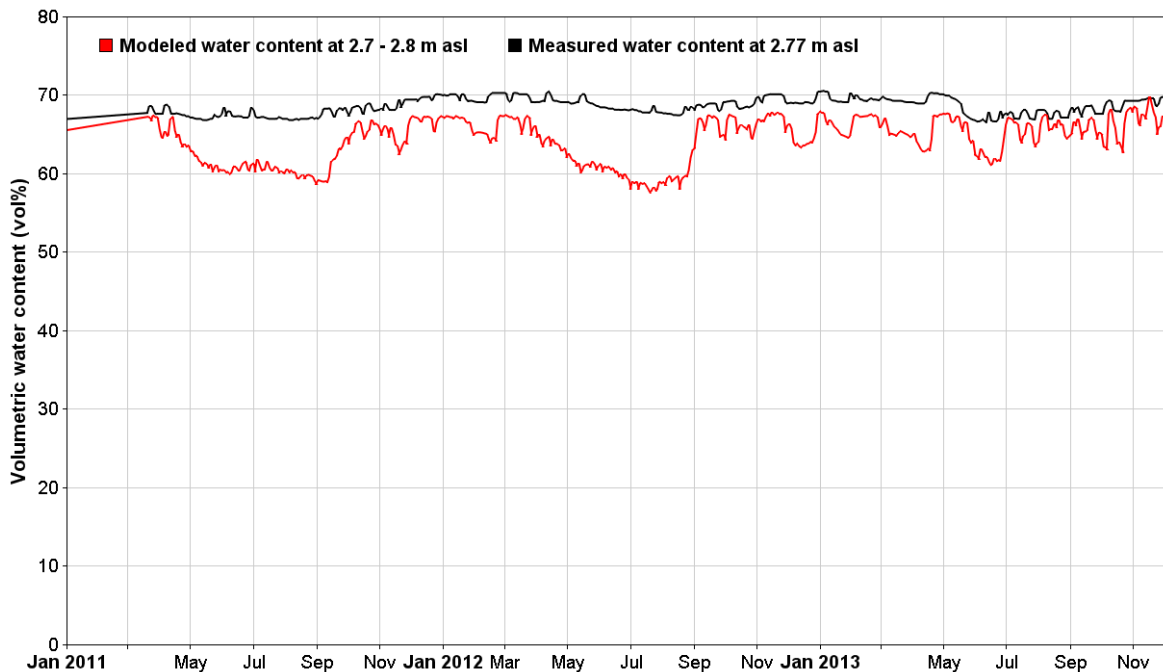


Figure 17: Measured and modeled water content in the lime/sand layer in a depth of about 1.2 m.

With an r^2 value of 0.14 for the lower cultural layer, it could be expected that the fit is very poor, but a RSME of 1.25 vol% and a visual comparison of the water content curves over time, show a satisfying fit (Figure 18). The measured time series shows a smooth curve below

70 vol% that slightly varies with the seasons. Considering the highly variable saturation level (see Figure 5) underneath and the corresponding pressure changes, the water content remains remarkably steady. The modeled time series shows a more "shaky" curve that indicates the influence of pressure variations. It was possible to calibrate the model in a way, that the dynamics of the water content are reproduced better, but it required unreasonably large modifications of measured soil properties and caused deterioration of modeled water content curves further up in the soil profile. However, the residuals are so small anyway, that further fitting of the curve did not seem reasonable.

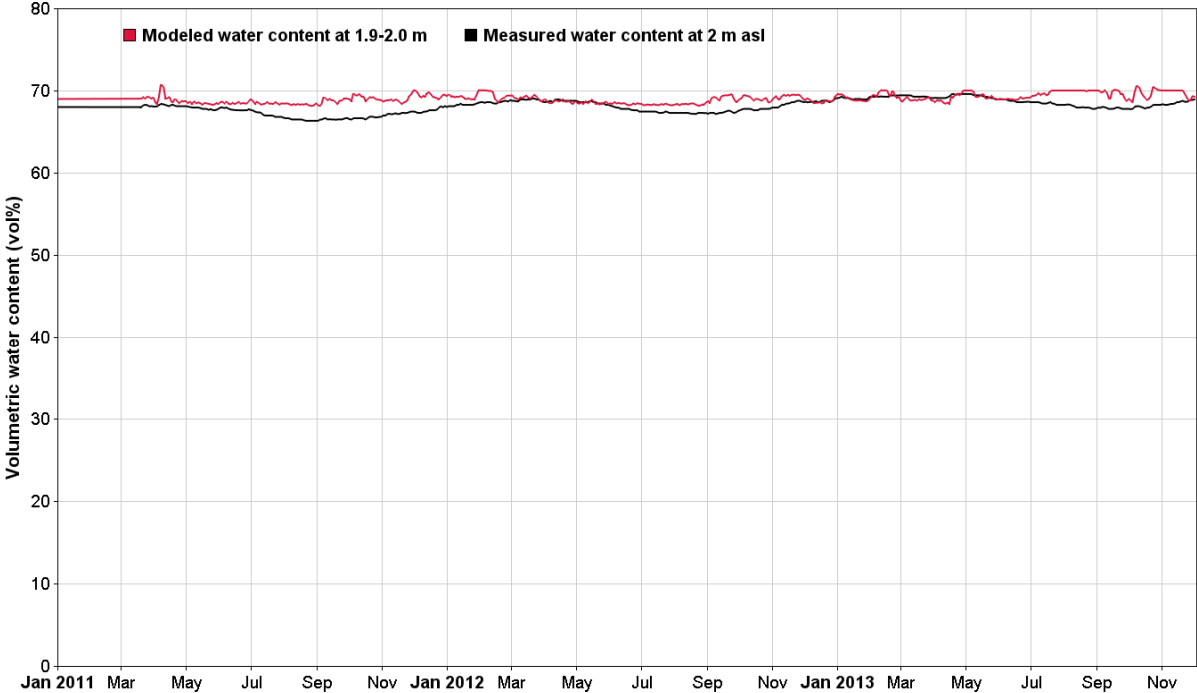


Figure 18: Validation of the modeled water content in the lower cultural deposits.

4.2 Water balance

Generally, the hydrologic water balance can be described by the equation $P = E + D + R - \Delta S$, where P is precipitation, E is evaporation, D is drainage, R is surface runoff, and ΔS is the change in water storage within the profile.

As mentioned in chapter 4.1.2, the first years of the model were run with a soil cover, which simulates a physical barrier for infiltration. In 2012, the infiltrability of the pavement was improved, so the simulations were continued without a physical barrier covering the testpit. The increased infiltrability of the soil changed the water balance considerably. The development over the years is visualized in Figure 19 and Figure 20. During the first five years, the proportions of runoff, evaporation and drainage remain relatively constant, and then changed dramatically in the course of 2012.

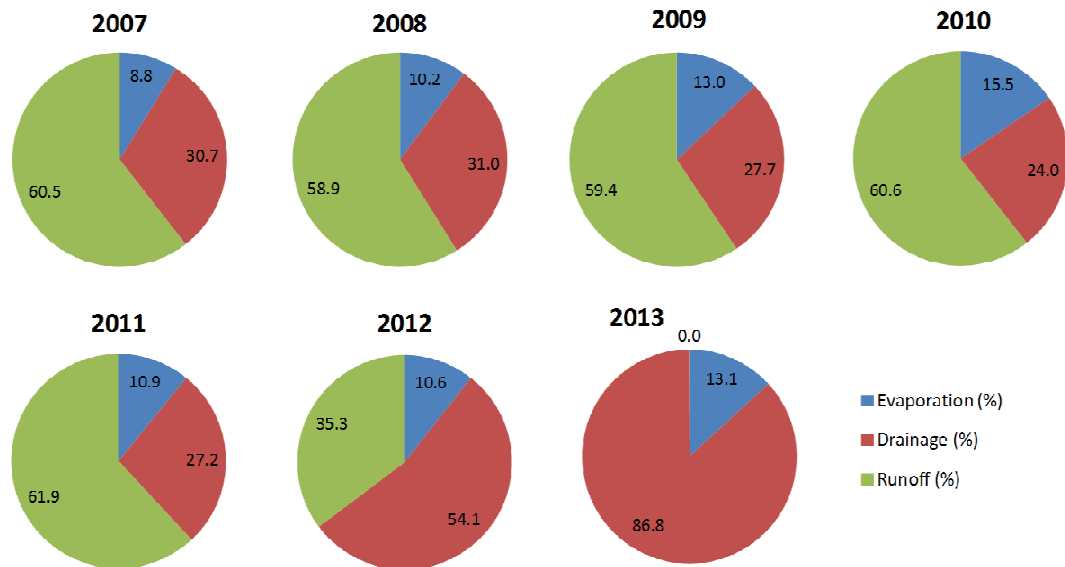


Figure 19: Simulated percentage of precipitation that evaporates, runs off, or infiltrates and drains in individual years from 2007 to 2013.

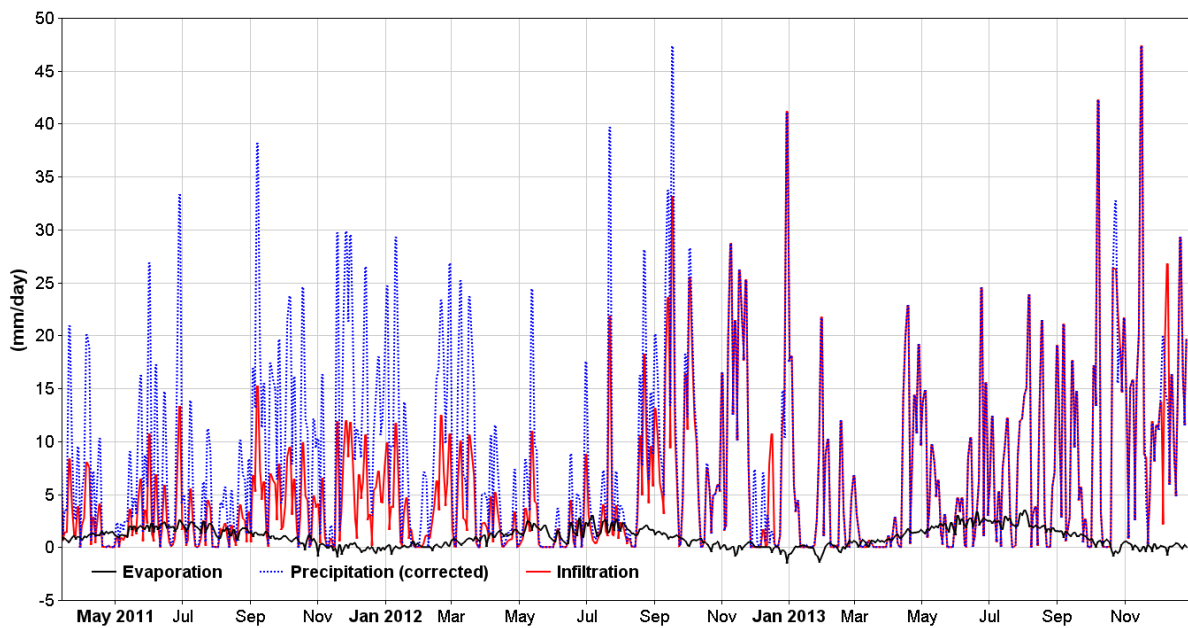


Figure 20: Corrected precipitation, simulated infiltration and evaporation from April 2011 to December 2013.

Based on Figure 21, several clues regarding the behaviour of the soil can be retrieved: It is apparent that the overall change in water storage is highly dependent on the season. Roughly spoken, the soil profile depletes for water in summer and replenishes in winter. This phenomenon is mainly caused by increased soil evaporation during the summer months (Figure 22). Higher precipitation rates in the autumn / winter months may also play a role.

It can also be seen, that the total difference in water content compared to the beginning of the simulation period is mostly negative. Minima between -100 and -125 mm reflect how severe the drying process in the summer months can be. Altogether, the water storage in the soil

profile in summer can be more than 150 mm less than during winter. It is these large variations in water storage that present a threat to the organic deposits of Bryggen.

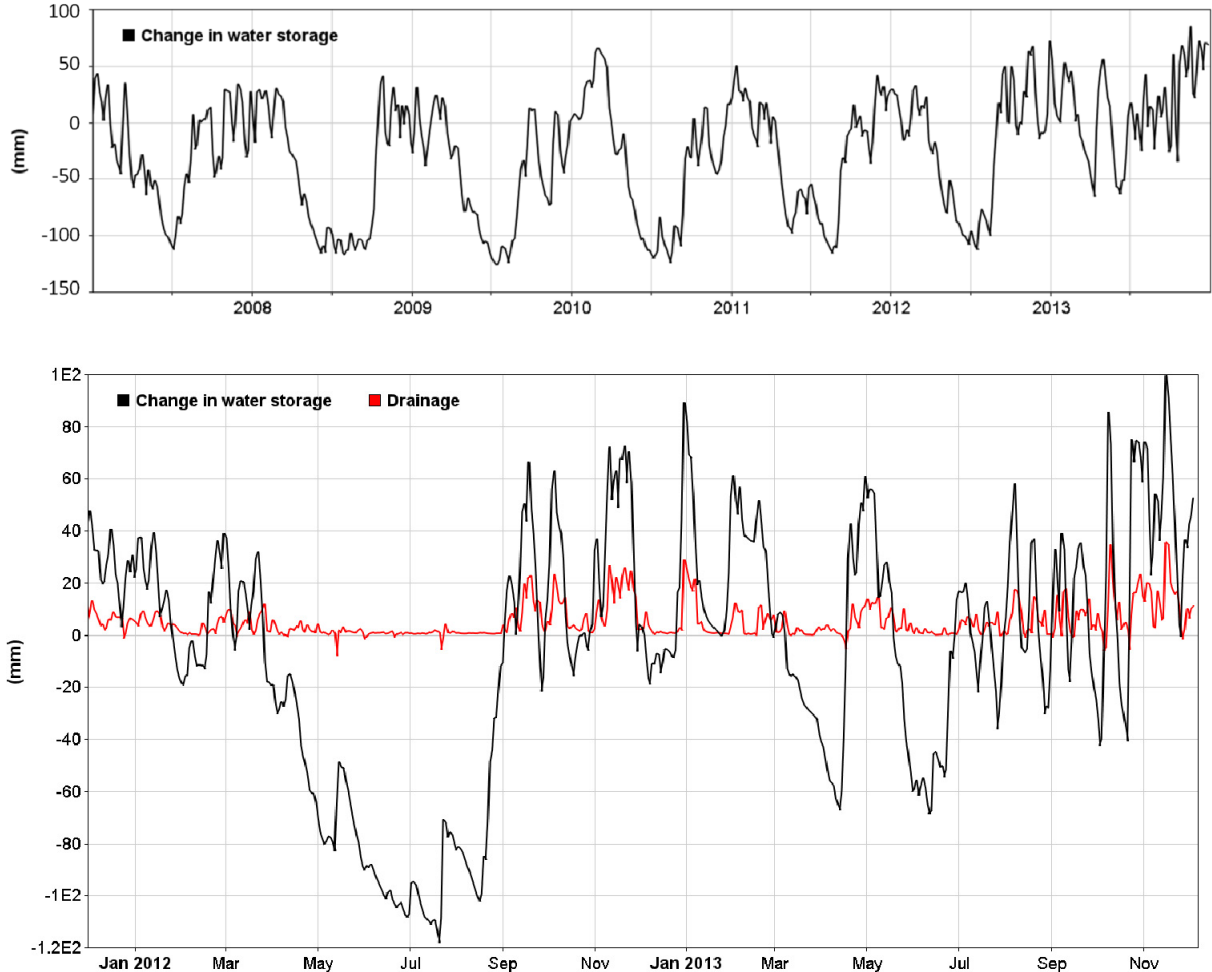


Figure 21: The total difference in water storage (mm) in the soil profile from 2007 to 2013 (upper graph), with January 2007 being the reference point. The lower graph shows the changes in water storage (mm) together with the drainage flow rates (mm/day) for the last two years of the modeling period.

In Table 3 average values of the total difference in storage for the individual years are listed. Both here and in Figure 21, the year 2013 differs considerably from all the others. The average water storage is approximately +11 mm more than in the beginning of the modelling period. With respect to the mentioned seasonal changes, January 2007 might not be the ideal reference point, even though it marks the beginning of the simulations. That in mind, the soil column contained on average approximately 60 mm of water more in 2013 than in other years.

The overall average value for drainage was simulated to be 2.9 mm/day, meaning that approximately 3 L of water are lost from a soil column with a surface area of 1 m² per day, or 0.125 L per hour. However, there are large differences between summer and winter. During summer, drainage reduces to less than 1 mm/day (Figure 22), or 0.04 L per hour and m². The discrepancy between the different time periods reflects the fact that infiltration increased substantially due to various physical measures at the site. In order to compensate for the deficit in water content and compared to average conditions in the soil, at least 0.08 L would need to be injected per hour and m² during the summer months.

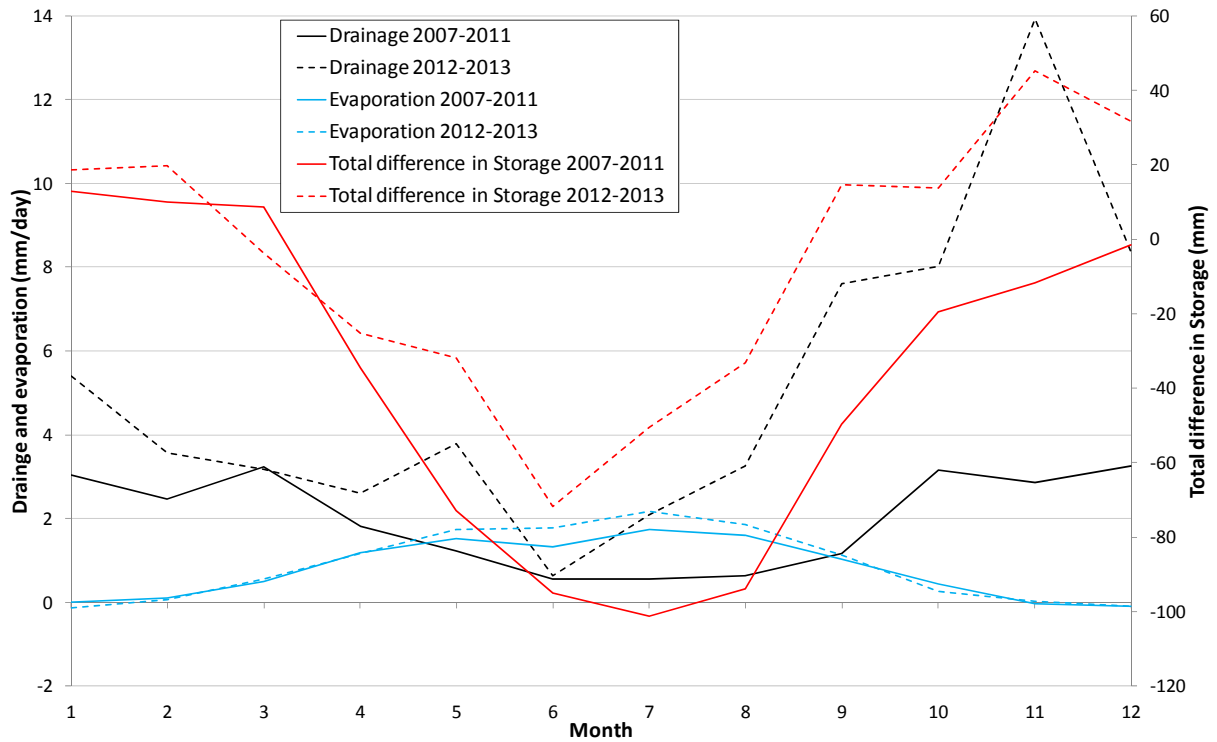


Figure 22: Monthly average values for evaporation (mm/day), drainage (mm/day) and the total difference in storage (mm) compared to January 2007. In order to visualize the effect of increased infiltration in the last 1.5 years on average values, two different periods are compared.

Table 3: The averaged changes in water storage in the soil (mm) in 2007-2013. Negative values indicate overall loss of water from the soil during that period, while positive values indicate replenishment.

	2007	2008	2009	2010	2011	2012	2013
Average total difference in water storage compared to January 2007 (mm)	-27.3	-46.3	-48.8	-36.3	-29.1	-23.0	10.7

4.3 Evaluation of errors and model constraints

The soil samples used for characterization of the modeled profile were gathered at different times and at slightly different localities. Considering the unusual heterogeneity of the local subsurface, it is hard to tell to what extent deviations between the measured and simulated variables might be due to insufficient quality of the soil data. Furthermore it is difficult to assess, how much the initial opening of the testpit in 2006 as well as the re-opening in 2010 have disturbed the initial layering and the natural water flow in the soil.

One major outcome of the CoupModel simulations was, that traditional soil sampling and analyses supply insufficient data input for infiltration simulations of urban soils. Functions for estimation of hydraulic conductivity and water retention curves are based on the inorganic, < 2 mm fraction of the soil. Urban soils however, are typically composed of highly disturbed materials of various origin. They do not necessarily reflect the local geology and climate, but rather present an archive of human history of the area. Accordingly, their physical, chemical and biological properties can differ entirely from soils that have grown naturally over a long period of time. An undisturbed forest soil has an organic horizon at the very top that gradually decomposes and becomes mixed with inorganic soil particles further down. The typical top horizon of an urban soil is not composed of organic materials, but of highly compacted inorganic materials, and is typically covered by cobblestone or asphalt. However, in cities such as Bergen, Oslo or Amsterdam, organic materials often play a role further down. Wooden foundations and other organic remains of various age, size, composition and degree of decomposition in the subsurface are not an exception. These organic materials influence the hydraulic properties of the soil considerably. However, depending on their volume, position, alignment, and degree of decomposition, their properties are highly variable. Loss on ignition values for extracted soil samples cannot account for the complexity of organic materials and their respective influence on the soil water retention curve.

Similar challenges are met with respect to gravel and other coarse, inorganic materials. The > 2 mm proportion of a soil is not included in any of the traditional equations for the estimation of hydraulic properties. Urban soil such as that at Bryggen contains a high proportion of gravel, stones and fragments of building materials. An estimation of soil hydraulic properties that is based on the grain size distribution of the inorganic, < 2 mm proportion of the soil only, will in most cases lead to an erroneous or at least incomplete description of the soil profile.

For the same reasons, it is difficult to apply literature values as compensation for missing measurement data. Soils are highly complex structures and it is not a trivial task to find a soil that satisfactorily resembles another soil in composition, degree of decomposition and compaction, layering, preferential flow paths through cracks or animal tunnels, and so on.

The total porosity of the lower, cultural layer had to be reduced from 80 to 70vol%, in order to make an appropriate fit of measured and modeled values. This modification seemed reasonable for the performed simulations, it may however lead to problems, if the model is used to simulate other processes than currently included.

The study site is surrounded by buildings, which block the sun at times. Accordingly, the net radiation may have been lower than estimated. Also, the soil's surface has a slight slope, which is currently not included in the model. A slope leads to changes in runoff and infiltration, and tilted horizons further down can cause a change in the flow path of infiltrating water.

It would have been desirable to use meteorological data from a station in close proximity to the study site. The station Bergen Florida lies about 2 km away, which sounds reasonably close. However, for a city like Bergen, where precipitation often occurs very local and its intensity may differ considerably from one place to another, local data series are advantageous. In July 2012, a local weather station was installed on the roof of Bryggen museum. Because the data did not cover the whole modelling period, data from Florida were used. In retrospect it might have been a good compromise, to use local precipitation data for the time period available, and combine them with the time series of the other station for the first 5.5 years.

5. Recommendations

As discussed in previous chapters, the knowledge about physical soil properties such as grain size distribution and the amount of organic material present in the soil is not sufficient for satisfying water content simulations of urban soil.

For future simulations of water content at urban sites it should be noted, that the derivation of soil water retention curves by direct measurements of the volumetric soil water content and the matric potential of undisturbed samples, is thought to be more appropriate than the use of basic physical properties. Several methods are available to investigate the connection between soil water potential and water content and all of them have their advantages and disadvantages. Commonly used apparatus are pressure plates or pressure flow cells. In order to obtain realistic results, soil samples should be undisturbed, intact cores. It can be assumed, that the method would deliver a better dataset for simulation purposes, but there are many disadvantages, that must be considered as well. In praxis, it could be a major challenge to obtain undisturbed and representative soil samples from all relevant horizons of urban soils. It is a time consuming procedure and there are various researchers that identified flaws of the method (see for example Bittelli and Flury, 2009)

Possibly the most representative technique for determination of soil water characteristic curves might be an in-situ sensor-pairing method, where TDR probes and pressure transducer tensiometers are installed in the soil at close proximity to each other. This way, the volumetric water content and the pore water pressure can be monitored simultaneously as the soil wetness varies and a soil water characteristic curve can be derived. The method is not without flaws either.

It is challenging to place the sensors in a way that allows for representative data collection and the initial calibration process can be difficult. However, so far, this might be the most appropriate method available to determine soil water characteristic curves for urban settings. Future studies similar to the case Bryggen should therefore include this sensor-pairing method in field investigations.

6. References

- Beven, K. J., and A. M. Binley (1992), The future of distributed models: Model calibration and uncertainty prediction, *Hydrol. Processes*, 6, pp. 279–298
- Bitteli, M., Flury, M. (2009) Errors in Water Retention Curves Determined with Pressure Plates. *Soil Science Society of America Journal*, Vol 73 (5)
- Brooks, R. H. & Corey, A. T., 1964: Hydraulic properties of porous medi. *Hydrology Paper No. 3*, Colorado State University, Fort Collins, Colorado, 27 pp.
- De Beer, J. (2008), Statusrapport grunnvannsovervåking og hydrogeologisk modellering ved Bryggen i Bergen, NGU report 2008.069 (in Norwegian only)
- De Beer, J.; Matthiesen, H. (2008), Groundwater Monitoring and Modelling from an Archaeological Perspective: Possibilities and Challenges. NGU Special Publication, 11, pp- 67-81.
- De Beer, J.; Price, S. J.; Ford, J. R. (2012), 3D modelling of geological and anthropogenic deposits at the World Heritage Site of Bryggen in Bergen, Norway, *Quaternary International*, 251, pp. 107-116
- Dunlop; R. (2008), The Bryggen Monitoring Project, Part 6: report on the archaeological investigation of three dipwell boreholes, Bryggen, 2006. NIKU report 63-2008, Bergen
- Hooghoudt, S. B. (1940), Bijdragen tot de kennis van enige natuurkundige grootheden van de ground. *No. 7 Versl. Landb. Onderz.* 42, pp. 449-541.
- Jansson, P.-E.; 2012, CoupModel: Model use, calibration, and validation, *American Society of Agricultural and Biological Engineers*, Vol. 55 (4)
- Jensen, J. A. (2007), Setningsmålinger på Bryggen i Bergen, Multiconsult report 610694, 7 pp. (in Norwegian only)
- Konzelmann, T.; van de Wal, R. S. W.; Greuell, W.; Bintanja, R.; Henneken, E. A. C. and Abe-Ouchi, A. (1994), Parameterization of global and long wave incoming radiation for the Greenland ice Sheet. *Global and Planetary Change*, 9, pp. 143-164
- Matthiesen, H. (2007). Preservation conditions above the groundwater level at Bugården, Bryggen in Bergen. Results from MB21 and a testpit from September 2006. Copenhagen: National Museum of Denmark, Department of Conservation, report nr. 10832-0011-1.
- Matthiesen, H. (2010). Preservation conditions in the area bordering the sheet piling at Bryggen, Bergen: Results from new dipwells MB15, 30, 31, 23 and MB33 installed in 2009. Copenhagen: National Museum of Denmark, Department of Conservation, report nr. 11031041.
- Matthiesen, H., Dunlop, R., Jensen, J.A., de Beer, H. & Christensson, A. (2008). Monitoring of preservation conditions and evaluation of decay rates of urban deposits - results from the first five years of monitoring at Bryggen in Bergen. *Geoarchaeological and Bioarchaeological Studies*. VU University Amsterdam, [10], pp. 163-174.
- Matthiesen, H.; Hollesen, J. (2011), Preservation conditions in unsaturated urban deposits: Reopening of testpit from 2006 and installation of monitoring equipment at the rear end of Nordre Bredsgården, Bryggen in Bergen. Copenhagen: National Museum of Denmark, Department of Conservation, report no 11031047
- Melling, L., Katimon, A., Joo, G. K., Uyo, L. J., Sayok, A., Hatano, R. (2007) Hydraulic conductivity and moisture characteristics of tropical peatland - preliminary investigations.
- Mualem, Y., 1976: A new model for predicting the hydraulic conductivity of unsaturated porous media. *Water Resour. Res.* 12:513-522.
- Rawls, W.J.; Pachepsky, Y.A.; Ritchie, J.C.; Sobecki, T.M.; Bloodworth, H. (2003); Effect of soil organic carbon on soil water retention, *Geoderma* 116, pp 61-76
- Stedinger, J. R., Vogel, R. M., Lee, S. U., Batchelder, R. (2008) Appraisal of the generalized likelihood uncertainty estimation (GLUE) method. *Water resources Research*, Vol 44, W00B06

Acknowledgements

The construction of the soil-water storage model for Bryggen was partly financed by the Research Council of Norway, the Directorate for Cultural Heritage and NGU.

Many people have been involved in the course of this work, such as Wieslawa Koziel (NGU), who conducted the laboratory analyses, and Per-Erik Jansson (KTH), who gave technical advice during the modelling work. Discussions and other contributions such as ideas, suggestions and critical questions by Hans de Beer, Henning Matthiesen, Bjørn Frengstad, Rory Dunlop and Jørgen Hollesen were highly appreciated.

APPENDIX

Table A 1: Soil samples collected 3.4.2013 in between the testpit US1 and the observation well MB21.

Sample No.	Depth (m)	Corresponds to horizon ¹	Comment
1	0.6 - 0.75	1	Sandy, no organics, a few stones
2	0.75 - 0.9	4	Medium grained sand
3	0.9 - 0.95	5	Mainly sand, contains large wooden pieces with signs of decay, moist
4	1.1 - 1.35	8	Black, wet, sandy, highly organic
5	1.35 - 1.75	9,10, 11	Dark, wet, loam
6	1.75 - 1.9	12	Dark, wet, sandy, contains stones
7	1.9 - 2.0	13	Sandy, contains coal
8	2.0 - 2.2	14	Moist, soft, dark, highly organic soil with wooden pieces
9	2.2 - 2.45	-	Very heterogeneous, containing both stones, lumps of clay and wooden pieces
10	2.55 - 2.8	-	Similar to sample 9

¹ after the description in Dunlop (2008)

Table A 2: Sample weights and soil water content

Sample No.	NGU's internal ID	Wet sample + plastic bag (g)	Wet sample (g)	Dry sample + plastic bag (g)	Weight loss \triangleq Mass of water (g)	% Weight loss (% Soil water)
1	82951	473.90	465.11	417.28	56.62	12.2
2	82952	274.00	265.21	229.60	44.40	16.7
3	82953	193.00	184.21	139.56	53.44	29.0
4	82954	549.74	540.95	399.8	149.94	27.7
5	82955	693.20	684.41	465.34	227.86	33.3
6	82956	758.10	749.31	578.92	179.18	23.9
7	82957	243.97	235.18	159.91	84.06	35.7
8	82958	351.10	342.31	140.28	210.82	61.6
9	82959	473.43	464.64	335.06	138.37	29.8
10	82960	482.68	473.89	349.42	133.26	28.1

Plastic bag: 8.79 g; relative analytical uncertainty at 1σ level: 8 %

Table A 3: Cumulative grain size distribution and coefficients of uniformity for the < 2 mm fraction

Particle diameter [μm]	No. 1 [wt%]	No. 2 [wt%]	No. 3 [wt%]	No. 4 [wt%]	No. 5 [wt%]	No. 6 [wt%]	No. 7 [wt%]	No. 8 [wt%]	No. 9 [wt%]	No. 10 [wt%]
< 0.6	0.32	0.34	0.22	0.39	1.26	0.69	0.66	0.65	0.25	0.29
< 2	2.87	3.26	2.26	3.74	9.15	5.36	5.34	5.36	2.26	2.64
< 5	5.85	6.46	4.59	9.26	18.2	11	10.9	11.2	4.82	5.63
< 6	6.68	7.18	5.13	10.9	20.6	12.5	12.4	12.9	5.54	6.46
< 10	9.44	9.25	6.81	16.1	27.6	16.9	17.3	18.2	7.95	9.27
< 15	12.2	10.9	8.4	21	33.2	20.7	21.8	23.1	10.3	12.1
< 20	14.7	12.2	9.77	25.2	37.8	23.9	25.6	27.3	12.4	14.8
< 25	17	13.4	11	28.8	41.5	26.7	28.8	31	14.4	17.2
< 50	25.5	18	15	39	51.7	35.2	38.3	43	21.5	26
< 60	28.2	20.3	16.3	41.7	54.5	37.8	40.9	46.5	23.9	28.8
< 63	29	21.1	16.7	42.5	55.3	38.6	41.7	47.5	24.6	29.6
< 70	30.8	23.1	17.6	44.3	57	40.2	43.4	49.7	26.1	31.3
< 75	32	24.5	18.3	45.4	58.2	41.3	44.5	51.1	27.1	32.4
< 90	35.1	28.9	20.1	48.2	60.9	44	47.4	54.7	29.7	35.3
< 125	40.7	38.8	26	53.3	65.3	48.9	52.6	60.9	34.5	40.2
< 200	53.1	62	51.8	64.1	72.2	57.6	61.8	70.7	42.1	47.3
< 250	60.3	74.5	69.2	69.4	74.8	61.5	65.9	74.5	45.2	50
< 400	71.8	88.1	90.6	78	79.4	69	73.7	82.1	52.2	56.6
< 500	76.4	89.9	93.6	82	82.1	73.5	78.3	86.8	57.2	61.3
< 600	78.8	90.9	94.3	83.7	84	76.2	80.5	88.4	61.1	64.9
< 1000	88.4	94.7	96.8	90.5	91.5	86.7	89.1	95.1	76.9	79.6
< 2000	100	100	100	100	100	100	100	100	100	100
C_u	23.8	14.9	10.3	31.5	38.0	55.2	38.0	28.7	35.1	45.8
Texture	Sandy loam	Loamy sand	Loamy sand	Sandy loam	Loam	Loamy sand	Sandy loam	Sandy loam	Loamy sand	Sandy loam

C_u = Coefficient of uniformity = d_{60}/d_{10}

Table A 4: Clay (< 2 μm) , silt (2-60 μm) , sand (0.06-2 mm), and gravel fractions (> 2 mm) of the soil samples

Sample No.	Clay %	Silt %	Sand %	Gravel %
1	1.6	14.6	41.3	42.5
2	3.0	15.7	73.4	7.9
3	2.0	12.2	72.6	13.3
4	2.3	23.2	35.7	38.8
5	7.1	35.3	35.4	22.1
6	3.1	18.9	36.2	41.9
7	3.8	25.4	42.2	28.6
8	5.1	39.3	51.1	4.5
9	1.0	9.1	32.1	57.8
10	1.6	15.9	43.1	39.4

Table A 5: General information, model structure, technical and numerical settings

	Option	Value
General	Start date	01.01.2007, 12:00
	End date	31.12.2013, 12:00
	Input time resolution	Daily mean values
	Output interval	30 min
	Number of iterations per day	96
	File name	Hyst_20890
Model structure	Evaporation	Radiation input style
	GroundWaterFlow	On
	HBV Soil Module	Off
	HeatEq	On
	Irrigation	Off
	LateralInput	Off
	Minteq	Off
	Nitrogen and Carbon	Off
	PlantType	No vegetation
	SaltTracer	Off
	SnowPack	On
SoilVapor	Off	
Technical settings	WaterEq	On with complete soil profile
	Likelihood function	Gaussian
	Marcov Chain Step	Exponential decrease
	PressureHeadSign	Negative
Numerical settings	ValidationOutputs	Only statistics
	FindTimeStep	No
	NumMethod	Forward difference
	TimeStepOption	Empirical

Table A 6: Parameter values at investigated horizons used for retention and conductivity calculations

Depth below soil surface (m)	Pore size distribution index λ	Air entry tension (cm)	entry ψ_a	Saturated soil water content θ_s (%)	Residual soil water content θ_r (%)	soil content	Macropore volume (%)	Saturated conductivity (med mer/d)	Turtuosity ks	Turtuosity parameter n
0 - 0.2	0.4764	13.9746	40	3.8891	4	920.4257	1			
0.2 - 0.8	0.4601	9.1202	45	3.9314	4	3157.999	1			
0.8 - 1.0	0.16	20	62	18	4	3128.004	1			
1.0 - 1.6	0.25	47	71	4.066	4	3343.808	1			
1.6 - 2.2	0.3602	10.3051	70	2.7713	4	350	1			

Table A 7: Switches and parameter settings with respect to meteorological data, radiation properties and soil evaporation.

Module	Switch/Parameter	Value
Meteorological data	CloudInput	Read from PG-file (first position)
	CommonRefHeight	Yes
	DBSunInput	Not Used
	PrecInput	Read from PG-file (first position)
	RadGlobInput	Estimated
	RadInLongInput	Estimated
	SweClimScenarios	No
	TempAirCycle	Annual
	TempAirInput	Read from PG-file (first position)
	TempSurfInput	Not used
	TrafficInput	off
	VapourAirInput	Read as pressure (first position)
	WSpeedInput	Generated by parameters
	AltMetStation	0
	HumRelMean	70
	PrecA0Corr /A1Corr	1.07 / 0.08
	ReferenceHeight	2
	Slope E-W	0
	Slope N-S	0
	TairLapseRate	0.0056
	TempAirAmpl	10
	TempAirMean	7.6
	TempAirPhase	0
	TempDiff_Index	1
	WindSpeedMean	2
	Radiation	LongWaveBalance
Turbidity		Constant
AlbSnowMin		40
AlbedoDry		24.8083
AlbedoKExp		1
AlbedoWet		11.3627
Emissivity		1
Latitude		60.4
RadFracAng1 / 2		0.22 / 0.5
Solar Time Adjust	0	
Soil Evaporation	Evaporation Method	PM-eq, Rs(3Par)
	Surface Temperature	Air Temperature
	MaxSoilCondens	2
	MaxSurfDeficit	-2
	MaxSurfExcess	1
	PsiRs_1p	200
RoughLBareSoilMom	0.001	

Table A 8: Switches and parameter settings with respect to soil and surface water

Module	Switch/Parameter	Value
Soil hydraulic	Conduct. funct.	Mualem
	Hydraulic funct.	Brooks & Corey
	Matric Conductivity	Function of total conductivity
	Pedo Functions	Not used
	Replace K-values	No
	Scaling retention	No
	Common value	10
	MinimumCondValue	1.00E-05
	SaturationDiff	0
	ScaleCoef Residual	1
	Sensitivity	0.5
	TempFacAtZero	0.54
TempFacLinIncrease	0.023	
Soil water flows	ConvectiveGasFlow	Off
	Crack	Bypass flow
	Hysteresis	On
	Initial water cond.	Uniform Pressure Head
	Soil Water Barrier	Off
	TransitTime Estim.	Off
	InitialGroundWater	-2.3
Drainage and deep percolation	DriveDrainLevel	Driving File
	Dynam. indexed file	off
	EmpiricalDrainEq	off
	LBoundSaturated	No flow
	PhysicalDrainEq	Hooghoudt Model
	Pump	off
	ReturnFlow	on
	DLayer	4
	DrainLevel	-2.3
	DrainSpacing	2
	GWSourceFlow	0
RadiusPipe	0.8	
Surface water	Furrow	Off
	PumpStation	Off
	RunOnInput	Off
	SP Max cover	1
	SPCovPot	1
	SPCoverTotal	50
	SoilCover	dynamic
	SurfCoef	0.8
	SurfPoolInit	0
	SurfPoolMax	0
	SurfPowerCoef	1

Table A 9: Snow and frost settings and parameters.

Module	Switch/Parameter	Value
Snow pack	NewSnowDensity	Linear f(air temp)
	SnowAdjustment	No correction
	SnowDensification	f(ice and liq. content)
	SnowPloughing	off
	SnowSurfTemp	Air Temperature
	AgeUpdatePrec	5
	AgeUpdatePrecThQ	0.9
	CritDepthSnowCover	0.01
	DensityCoefMass	0.5
	DensityCoefWater	200
	DensityOfNewSnow	100
	MeltCoefAirTemp	2
	MeltCoefGlobRad	1.50E-07
	MeltCoefReFreeze	0.1
	MeltCoefSoilHeatF	0.5
	OnlyRainPrecTemp	2
	OnlySnowPrecTemp	0
	SThermalCondCoef	2.86E-06
	SnowDepthInitial	0
	SnowMassInitial	0
WaterRetention	0.07	
ZeroTemp_WaterLimit	3	
Soil frost	Flow Domains	Low + High Domain
	FrostInteract	InfluencingWater
	FrostSwelling	On
	Infiltration	In Low FlowDomain
	LoadPotential	On
	k-estimate	MinimumValues
	AlphaHeatCoef	1000
	FreezePointF0	10
	FreezePointF1	0
	FreezePointFWi	0.5
	HighFlowDampC	5
	LowFlowCondImped	4
	MaxSwell	0.05
	ShrinkRateFraction	0.05

Table A 10: Soil thermal and heat flow settings and parameters.

Module	Switch/Parameter	Value
Soil thermal	SolidHeatCapDist	Uniform
	CFrozenMaxDamp	0.9
	CFrozenSurfCorr	0.2
	ClayFrozen C1-C4	0.00144, 1.32, 0.0036, 0.8743
	ClayUnFrozen C1-C3	0.13, -0.029, 0.6245
	Organic C1-C2	0.06, 0.005
	OrganicFrozenC	2
	OrganicLayerThick	0
	SandFrozen C1-C4	0.00158, 1.336, 0.00375, 0.9118
SandUnFrozen C1-C3	0.1, 0.058, 0.6245	
Soil heat flows	Analytical Solution	Off
	Convection flow	Accounted for
	Heat Pump	Not used
	Heat Source	Not used
	Initial Heat Cond.	Uniform temperature
	Insulated Water Pipe	Off
	Lower Boundary	Temperature Cycle
	PrecTemperature	Equal surface temperature
	Thermal Conduct.	Not as output
	SoilInitTempConst	10
	TempDiffPrec_Air	-2

Table A 11: Linear regression values (r^2 , intercept and slope), Mean Error values (ME), and Root Mean Error Values (RMSE) for the comparison of simulated and measured soil temperatures and water contents.

Height of sensor (m asl)	Measured Temperature / Water content	n	r^2	Intercept	Slope	ME	RMSE
4.12	T	47608	0.89	0.49	0.92	0.23	1.87
3.92	T	47608	0.90	-0.05	0.94	0.56	1.79
3.68	T	47608	0.97	-0.25	1.03	0.04	0.81
3.46	T	47608	0.98	-0.17	1.02	-0.04	0.68
3.21	T	47608	0.98	-0.10	1.03	-0.17	0.61
3.06	T	47608	0.98	-0.66	1.11	-0.22	0.71
2.77	T	47608	0.97	-0.37	1.10	-0.47	0.84
2.5	T	47608	0.95	-0.22	1.09	-0.49	0.86
2.31	T	47608	0.92	-0.17	1.09	-0.54	1.03
3.92	W	42582	0.49	10.14	0.57	0.78	5.11
3.6	W	2389	0.05	32.55	0.20	-10.61	10.97
3.09	W	34877	0.27	-20.04	1.40	-1.62	4.57
2.77	W	47592	0.36	54.35	0.22	-4.19	4.84
2	W	47592	0.14	32.31	0.52	0.95	1.25

Table A 12: Soil cover dynamics

Date	SoilCover¹
01.01.2007	0.6
15.03.2012	0.55
01.06.2012	0.52
11.06.2012	0.5
13.07.2012	0.45
02.08.2012	0.4
13.08.2012	0.35
11.09.2012	0.3
19.09.2012	0.2
24.09.2012	0.1
19.10.2012	0

¹ A physical barrier between 0 and 1 that governs how much precipitation will infiltrate into the soil

Table A 13: Hysteresis effects in different depths

Depth	HysMaxEffRet parameter¹
0-0.2	0.2
0.2-0.6	0.1
0.6-0.8	1
0.8-1.0	0.9
1.0-1.5	0.1
1.5-1.7	1
1.7-3.5	0.8

¹ Gives the maximum hysteresis effect on water retention

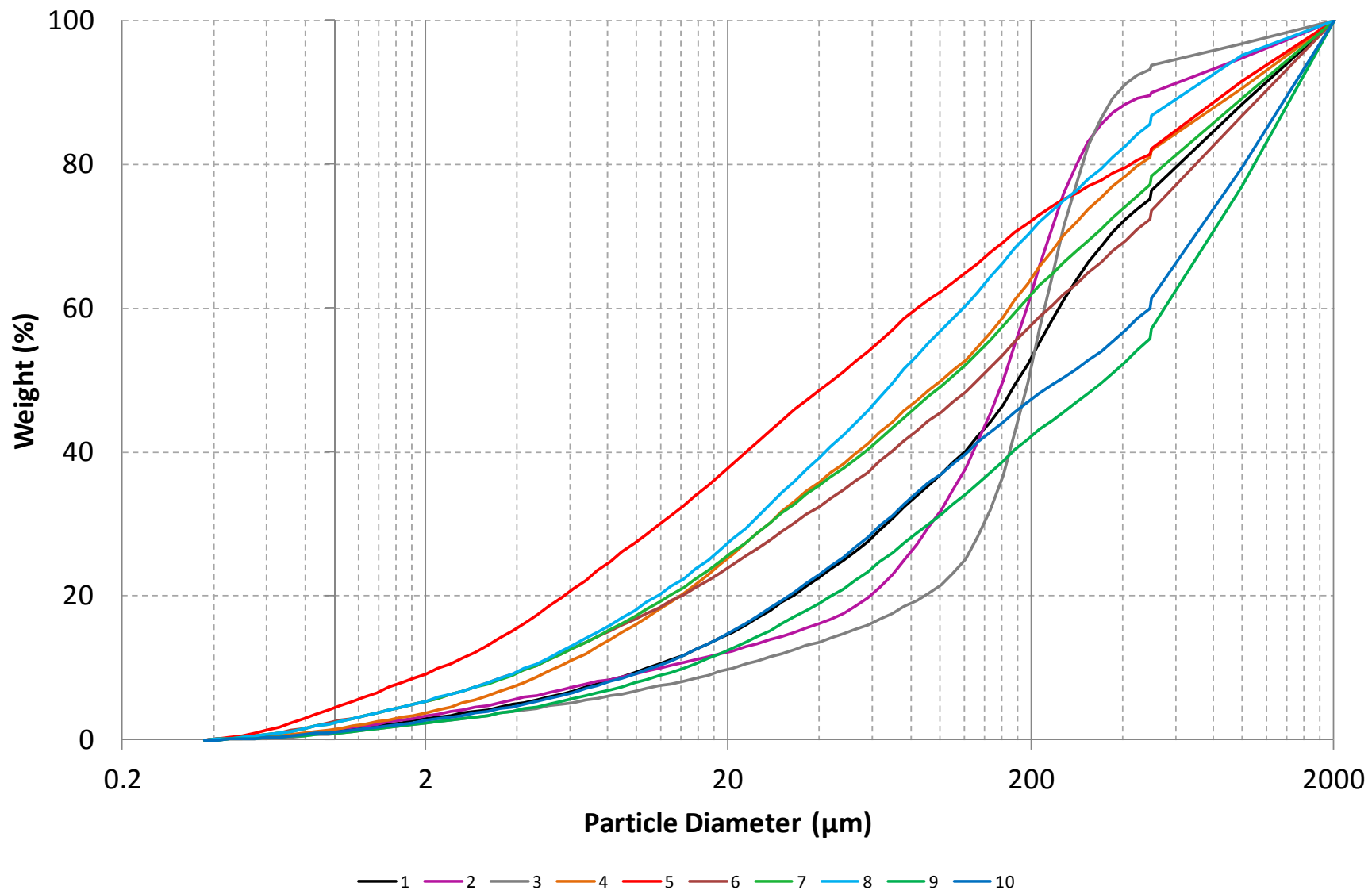


Figure A 1: Overview about the grain size distributions of the fine soil fractions

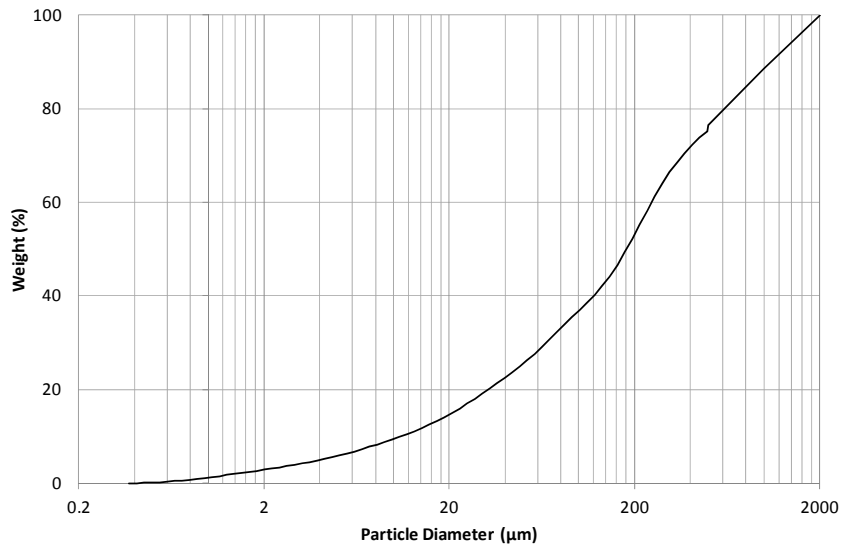


Figure A 2: Grain size distribution curve of soil sample 1. Texture class Sandy loam.

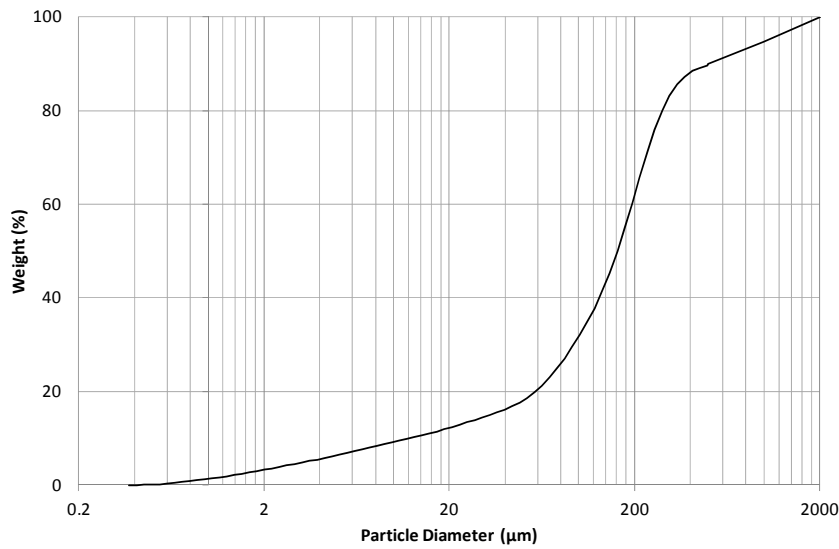


Figure A 3: Grain size distribution curve of soil sample 2. Texture class Loamy sand

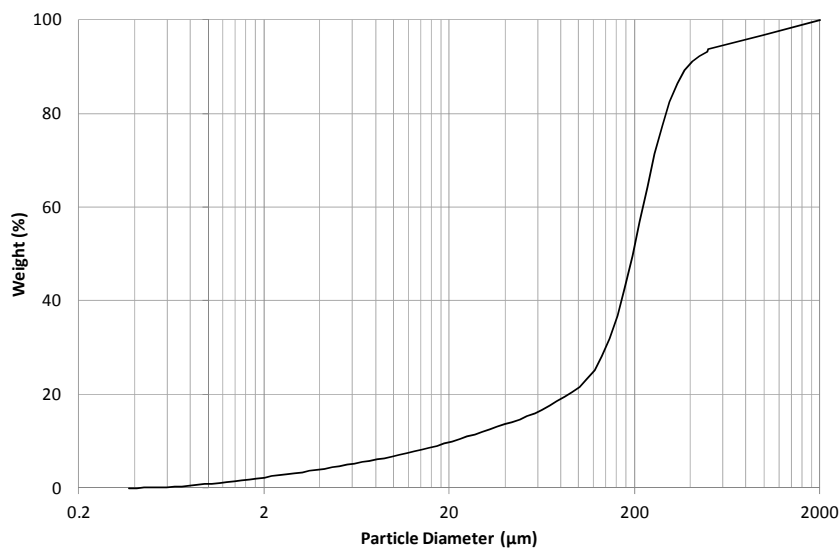


Figure A 4: Grain size distribution curve of soil sample 3. Texture class: Loamy sand.

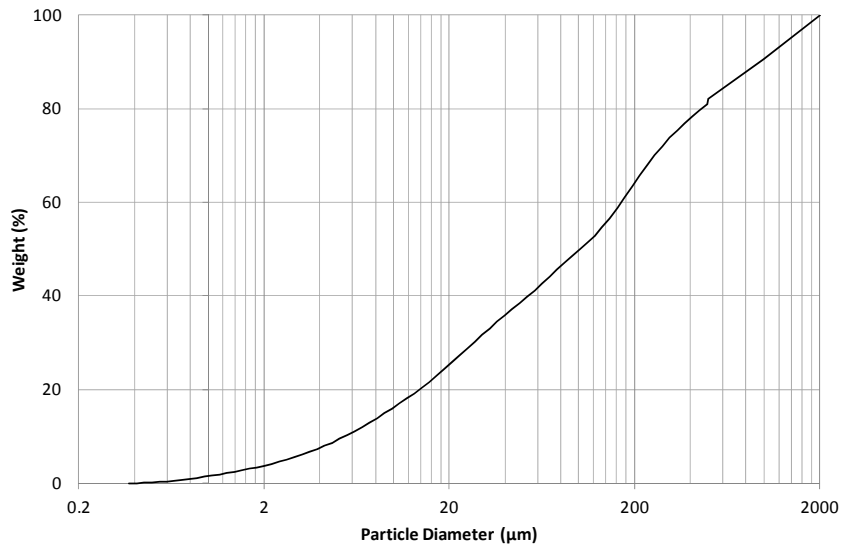


Figure A 5: Grain size distribution curve of soil sample 4. Texture class: Sandy loam.

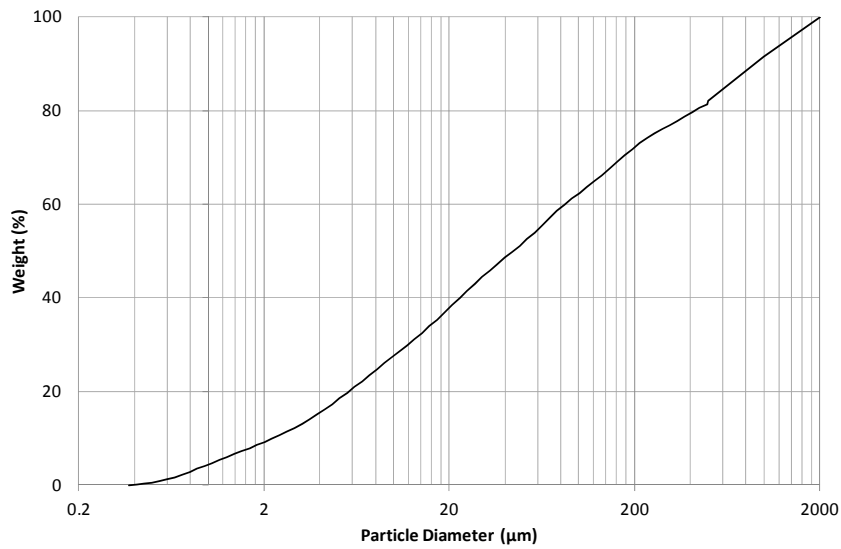


Figure A 6: Grain size distribution curve of soil sample 5. Texture class: Loam

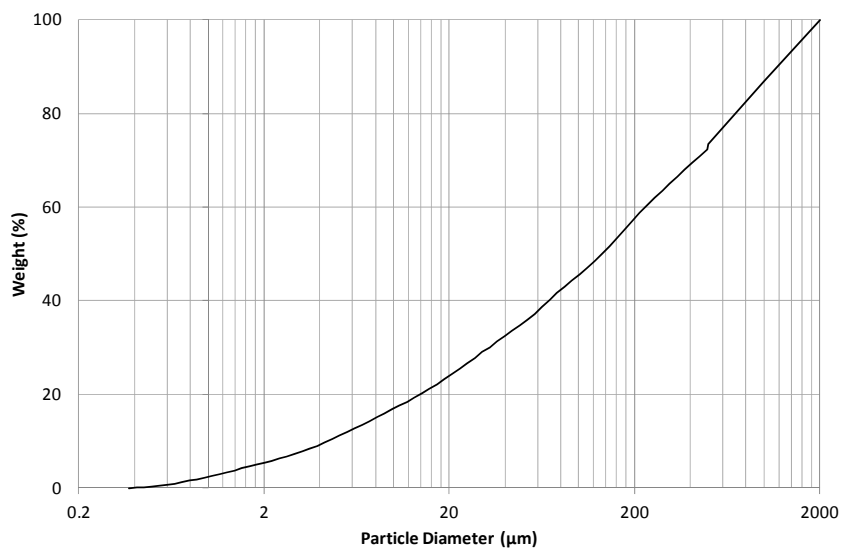


Figure A 7: Grain size distribution curve of soil sample 6. Textural class: Loamy sand

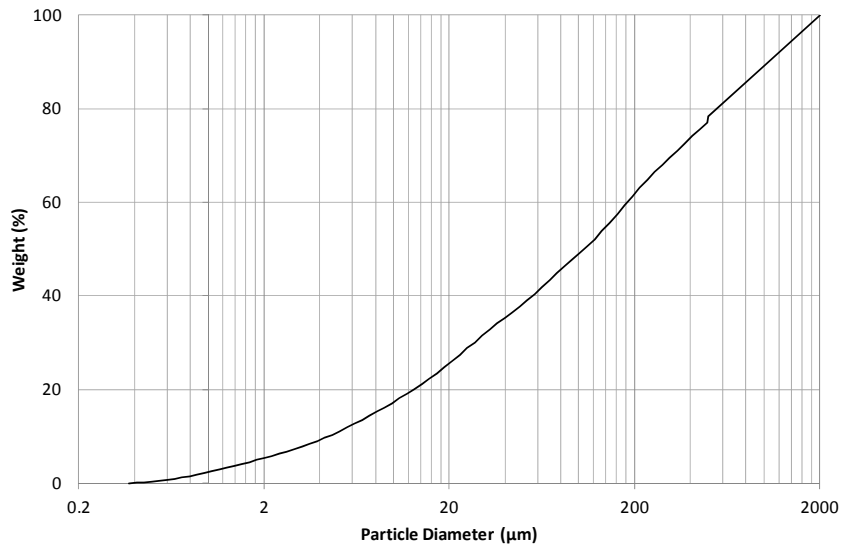


Figure A 8: Grain size distribution curve of soil sample 7. Textural class: Loamy sand

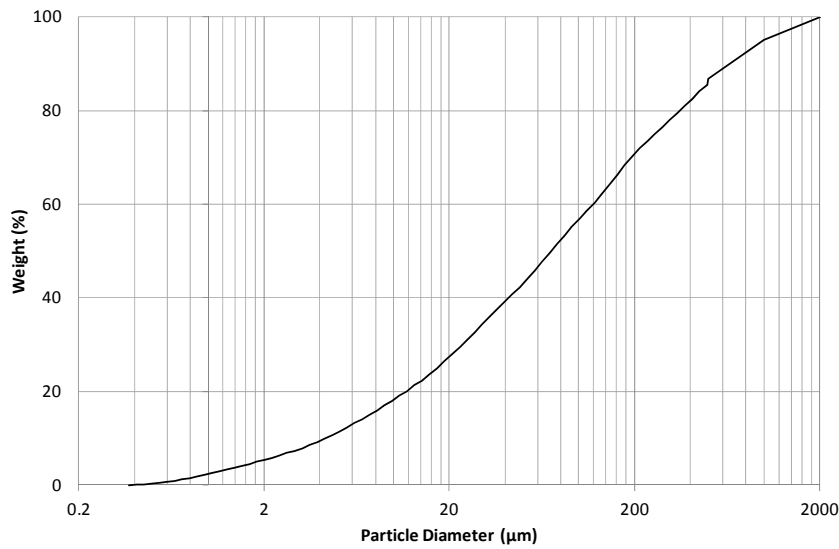


Figure A 9: Grain size distribution curve of soil sample 8. Textural class: Sandy loam

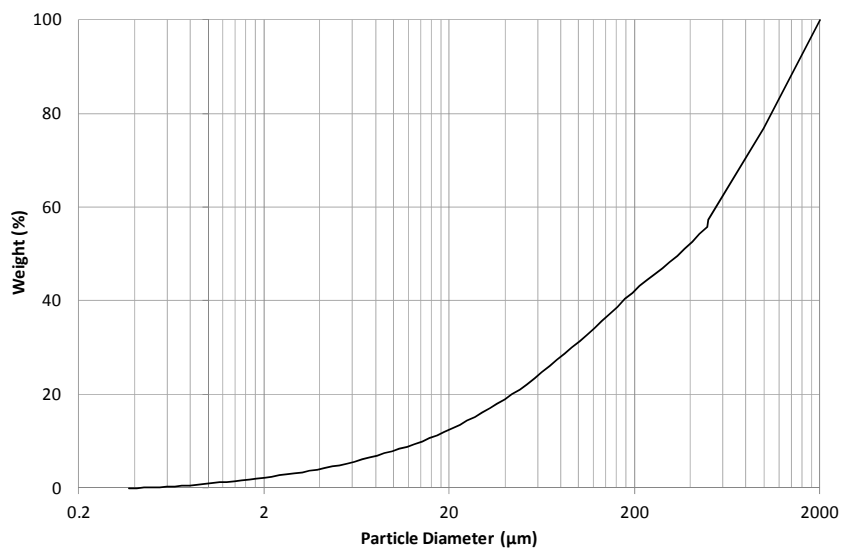


Figure A 10: Grain size distribution curve of soil sample 9. Textural class: Loamy sand

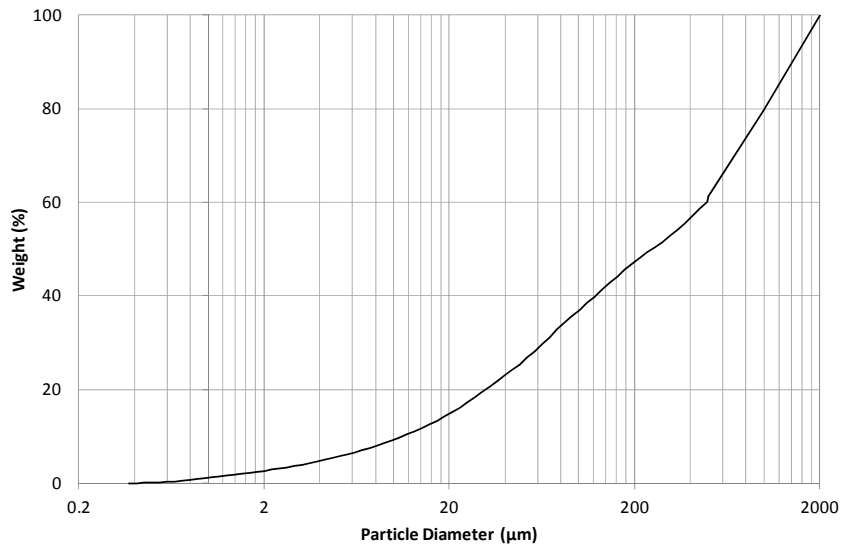


Figure A 11: Grain size distribution curve of soil sample 10. Textural class: Sandy loam

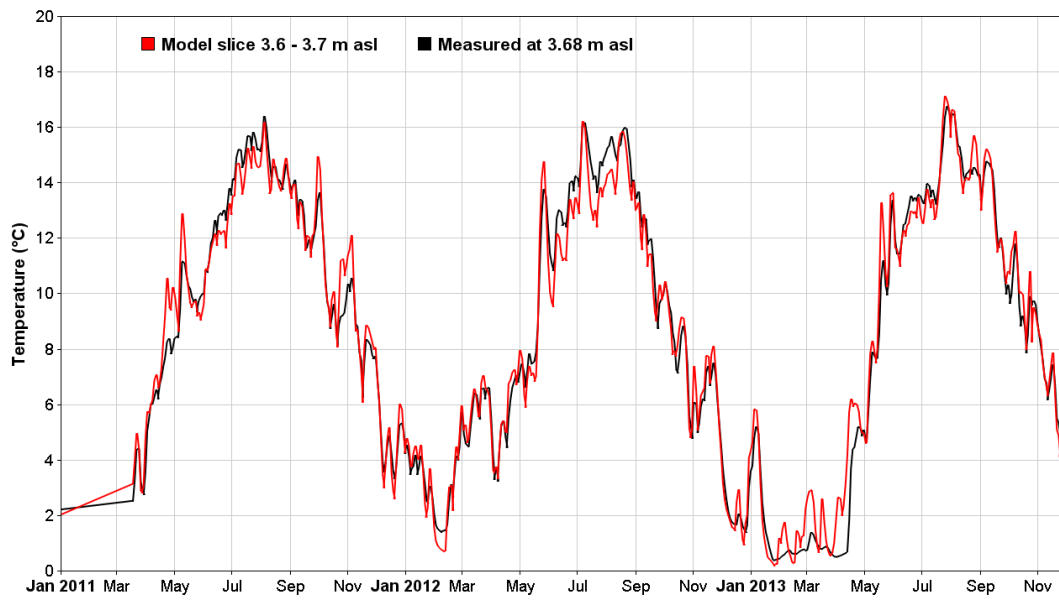


Figure A 12: Measured and modeled soil temperature at a depth of 0.3 - 0.4 m



Figure A 13: Measured and modeled soil temperature at a depth of 0.5 - 0.6 m



Figure A 14: Measured and modeled soil temperature at a depth of 0.7 - 0.8 m

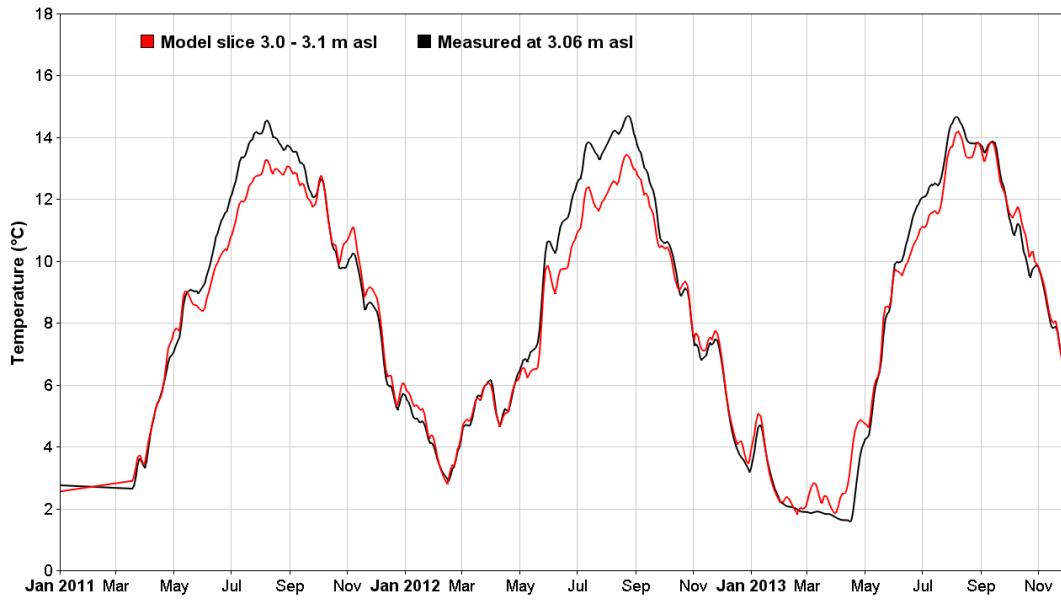


Figure A 15: Measured and modeled soil temperature at a depth of 0.9 - 1.0 m

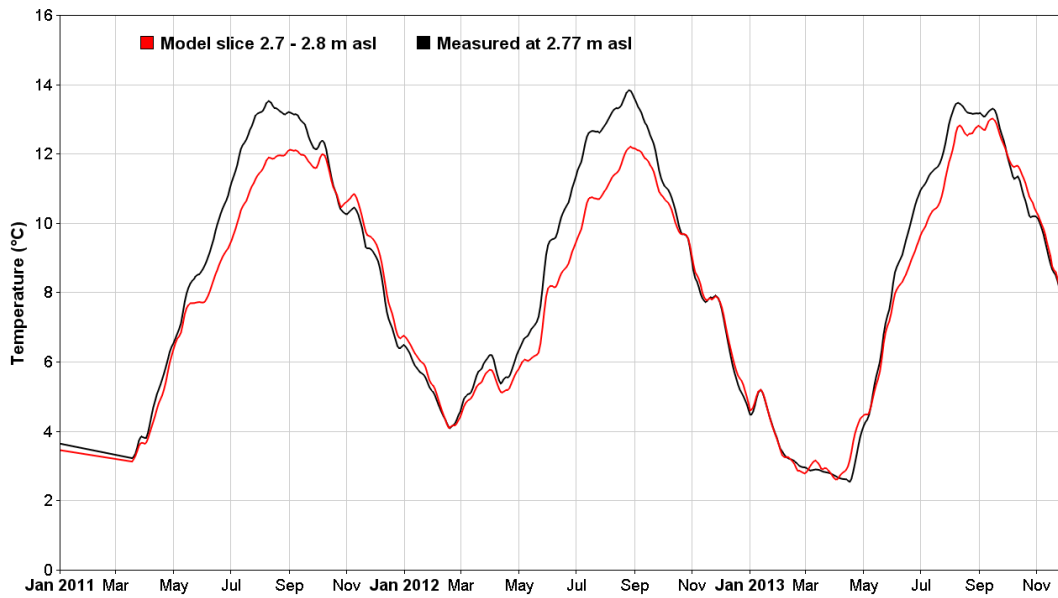


Figure A 16: Measured and modeled soil temperature at a depth of 1.2 - 1.3 m

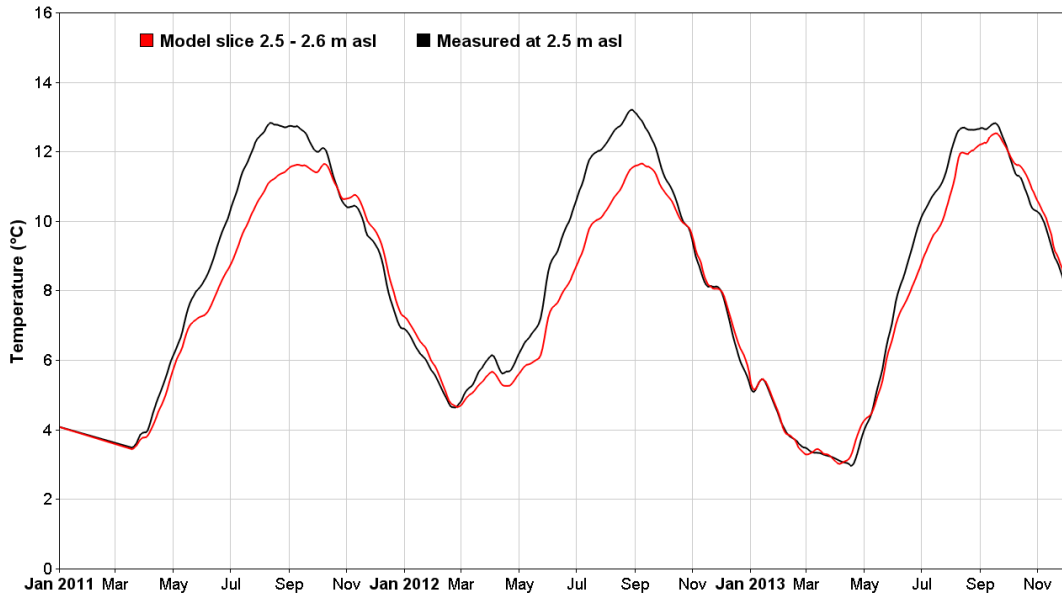


Figure A 17: Measured and modeled soil temperature at a depth of 1.4 - 1.5 m

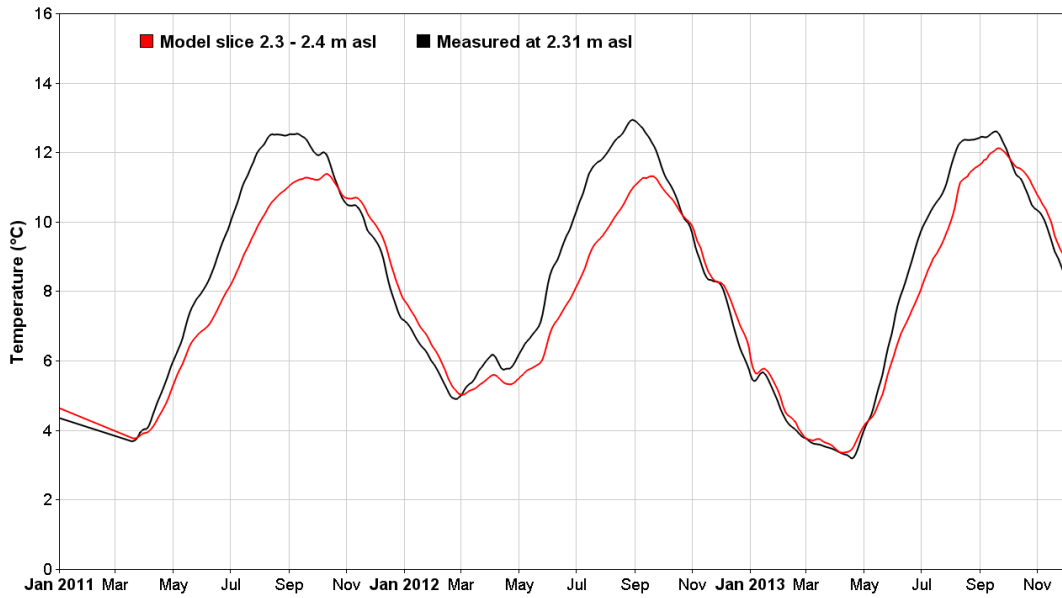


Figure A 18: Measured and modeled soil temperature at a depth of 1.6 - 1.7 m